ORIGINAL ARTICLE

MOLECULAR ECOLOGY WILEY

Faster-haplodiploid evolution under divergence-with-geneflow: Simulations and empirical data from pine-feeding hymenopterans ••

Emily E. Bendall¹ | Robin K. Bagley¹ | Vitor C. Sousa² | Catherine R. Linnen¹

²CE3C – Centre for Ecology, Evolution and Environmental Changes, Department of Animal Biology, Faculdade de Ciências da Universidade de Lisboa, University of Lisbon, Lisboa, Portugal

Correspondence

Vitor C. Sousa, CE3C - Centre for Ecology, Evolution and Environmental Changes, Department of Animal Biology, Faculdade de Ciências da Universidade de Lisboa, University of Lisbon, Lisboa, Portugal. Email: vmsousa@fc.ul.pt

Catherine R. Linnen, Department of Biology, University of Kentucky, Lexington, Kentucky, USA.
Email: catherine.linnen@uky.edu

Present address

Emily E. Bendall, Department of Microbiology and Immunology, University of Michigan, Ann Arbor, Michigan, USA

Robin K. Bagley, Department of Evolution, Ecology, and Organismal Biology, The Ohio State University at Lima, Lima, Ohio, USA

Funding information

Fundação para a Ciência e
a Tecnologia, Grant/Award
Number: CEECIND/02391/2017,
CEECINST/00032/2018/CP1523/CT0008
and UIDB/00329/2020; National Science
Foundation, Grant/Award Number: DEB1257739 and DEB-CAREER-1750946;
National Institute of Food and
Agriculture, Grant/Award Number:
2015-67011-22803; Faculdade de
Ciências e Tecnologia, Universidade Nova
de Lisboa, Grant/Award Number: CPCA/
A0/7303/2020; European Commission,
Grant/Award Number: 799729

Handling Editor: Christian Schlötterer

Abstract

Although haplodiploidy is widespread in nature, the evolutionary consequences of this mode of reproduction are not well characterized. Here, we examine how genomewide hemizygosity and a lack of recombination in haploid males affects genomic differentiation in populations that diverge via natural selection while experiencing gene flow. First, we simulated diploid and haplodiploid "genomes" (500-kb loci) evolving under an isolation-with-migration model with mutation, drift, selection, migration and recombination; and examined differentiation at neutral sites both tightly and loosely linked to a divergently selected site. As long as there is divergent selection and migration, sex-limited hemizygosity and recombination cause elevated differentiation (i.e., produce a "faster-haplodiploid effect") in haplodiploid populations relative to otherwise equivalent diploid populations, for both recessive and codominant mutations. Second, we used genome-wide single nucleotide polymorphism data to model divergence history and describe patterns of genomic differentiation between sympatric populations of Neodiprion lecontei and N. pinetum, a pair of pine sawfly species (order: Hymenoptera; family: Diprionidae) that are specialized on different pine hosts. These analyses support a history of continuous gene exchange throughout divergence and reveal a pattern of heterogeneous genomic differentiation that is consistent with divergent selection on many unlinked loci. Third, using simulations of haplodiploid and diploid populations evolving according to the estimated divergence history of N. lecontei and N. pinetum, we found that divergent selection would lead to higher differentiation in haplodiploids. Based on these results, we hypothesize that haplodiploids undergo divergence-with-gene-flow and sympatric speciation more readily than diploids.

KEYWORDS

faster-X, gene flow, genomic differentiation, haplodiploidy, local adaptation, speciation

Vitor C. Sousa and Catherine R. Linnen contributed equally.

¹Department of Biology, University of Kentucky, Lexington, Kentucky, USA

.365294x, 2022, 8, Downloaded from https://onlinelibrary.wiley.com/doi/10.1111/mec

16410 by Nationwide Children Hospital, Wiley Online Library on [01/03/2023]. See

for rules

1 INTRODUCTION

In terms of both species richness and biomass, haplodiploid organisms account for a substantial proportion of terrestrial biodiversity (Forbes et al., 2018; Hölldobler & Wilson, 1990). Haplodiploidy (arrhenotoky)—a reproductive mode in which females develop from fertilized eggs and are diploid, while males develop from unfertilized eggs and are haploid—has evolved repeatedly in diverse arthropod lineages and is present in an estimated 12% of extant animal species (Blackmon et al., 2017; de la Filia et al., 2015; Hedrick & Parker, 1997; Normark, 2003). From a theoretical perspective, most work on haplodiploidy has focused on the evolution of eusociality (Hamilton, 1964a, 1964b, 1972; Rautiala et al., 2019, but see Hartl, 1972; de la Filia et al., 2015). However, haplodiploid transmission genetics can have many other important evolutionary consequences. For example, when haplodiploid populations hybridize, only female hybrids are produced in the first generation and hybrid males are produced in the subsequent generation. This asymmetry may lead to higher rates of mitochondrial introgression compared to nuclear introgression (Linnen & Farrell, 2007; Patten et al., 2015) and may have consequences for the evolution of postzygotic isolation (Bendall et al., 2020; see also Ghenu et al., 2018; Nouhaud et al., 2020). Haplodiploidy is also expected to impact the evolution of sexually selected traits (Kirkpatrick & Hall, 2004; Reeve & Pfennig, 2003), mating systems (Boulton et al., 2015; Werren, 1993), parental care (Davies & Gardner, 2014; Gardner, 2012), sex ratios (Hamilton, 1967), and the outcomes of intra- and interlocus conflicts (Hitchcock et al., 2022; Klein et al., 2021; Kraaijeveld, 2009). However, formal theory and empirical tests for the evolutionary consequences of haplodiploidy remain rare (de la Filia et al.. 2015).

Here, we focus on how haplodiploidy affects genomic differentiation in diverging populations and species. Similarities in transmission genetics between haplodiploid genomes and X (or Z) chromosomes make it possible to draw on faster-X theory to generate predictions for haplodiploids (Avery, 1984; Hartl, 1972; Hedrick & Parker, 1997; Kraaijeveld, 2009). Within populations, hemizygosity in XY and haplodiploid males will expose recessive or partially recessive mutations to selection, thereby hastening the removal of deleterious alleles and the fixation of beneficial alleles (Avery, 1984; Charlesworth et al., 1987; Hedrick & Parker, 1997). More efficient selection on novel hemizygous alleles will also impact linked variation via hitchhiking (Betancourt et al., 2004) and background selection (Charlesworth, 2012), and these effects will be exacerbated by a lack of recombination in XY and haplodiploid males (Betancourt et al., 2004; Lester & Selander, 1979; Owen, 1986). As long as adaptation is driven primarily by new mutations that are at least partially recessive, faster-X theory predicts higher adaptive substitution rates and greater genetic divergence at linked sites on sex chromosomes and haplodiploid genomes relative to diploid autosomes when populations or species diverge in isolation (Presgraves, 2018, but see Wright et al., 2015).

Conversely, models of divergence-with-gene-flow via common genetic variants suggest that adaptive differentiation occurs more readily for sex-linked (or hemizygous) loci than for autosomal loci, regardless of dominance (Lasne et al., 2017). Instead, the magnitude of the faster-X effect on local adaptation depends on the rate of migration of the heterogametic sex relative to the homogametic sex. This is because when the genetic variants under selection are common, the efficiency of selection against maladapted immigrant alleles becomes more important than fixation of rare mutations (Lasne et al., 2017). Although the effects on linked variation have not, to our knowledge, been explored in the context of primary divergence-with-gene-flow models (e.g., Lasne et al., 2017), secondary contact models reveal that sex-limited hemizygosity and recombination can reduce effective migration rates at neutral loci linked to loci involved in local adaptation and/or hybrid incompatibilities (Fraïsse & Sachdeva, 2021; Fusco & Uyenoyama, 2011; Muirhead & Presgraves, 2016). Together, these models suggest that as long as gene flow accompanies divergence, sex chromosomes and haplodiploid genomes will tend to exhibit greater differentiation at selected and linked sites compared to autosomal chromosomes.

Consistent with faster-X theory, comparative and population genomic data from diverse taxa suggest that faster-X effects (i.e., elevated differentiation, divergence and substitution rates on sex chromosomes) are widespread in nature (Irwin, 2018; Meisel & Connallon, 2013; Presgraves, 2018). However, these patterns are not necessarily caused by sex-limited recombination and hemizygosity. Indeed, there are many other differences between sex chromosomes and autosomes that can also produce differences in genetic differentiation, including: differences in effective population size (N_a), mutation rate, recombination rate, gene content, sex-limited gene expression, and susceptibility to meiotic drive, sexual conflict and sexual selection (Frank, 1991; Hurst & Pomiankowski, 1991; Meiklejohn et al., 2018; Patten, 2018). Because they lack sex chromosomes, haplodiploids are potentially powerful models for investigating the impact of sex-limited hemizygosity and recombination on genomic differentiation independent of sex-chromosome-specific factors. However, because they also lack anything analogous to diploid autosomes, haplodiploids do not have a built-in benchmark for quantifying "faster-haplodiploid" effects, which we define as greater differentiation or divergence in haplodiploids relative to comparable diploids. Fortunately, increasingly sophisticated tools for simulating genomic data sets evolving under complex demographic and ecological scenarios (Hoban et al., 2012; Haller & Messer, 2019; Terasaki Hart et al., 2021) offer a strategy for evaluating the potential for faster-haplodiploid effects: simulate a benchmark diploid data set with equivalent demographic history, recombination and mutation under neutral and adaptive scenarios. We note that analogous to use of the term "faster-X effect" (Meisel & Connallon, 2013), we are using the term "faster-haplodiploid effect" to refer to an empirical pattern, without making assumptions about the underlying evolutionary mechanisms.

To better understand the impact of haplodiploidy on genomic differentiation, we combine simulations of haplodiploid and diploid genomes evolving under divergence-with-geneflow with an empirical case study of a haplodiploid species pair for which we have extensive knowledge regarding the drivers of divergent selection and reproductive isolation, as well as basic life history knowledge to parameterize simulations. Neodiprion pinetum (white pine sawfly) and N. lecontei (redheaded pine sawfly) are sister species with overlapping distributions in eastern North American (Linnen & Farrell, 2008, 2010). Because both species are pests of economically important pines, their basic ecology and life history are well described (Benjamin, 1955; Coppel & Benjamin, 1965; Knerer & Atwood, 1973; Rauf & Benjamin, 1980; Wilson et al., 1992). Reproductive adults emerge in spring after overwintering as prepupae in cocoons. Females fly to their preferred host and attract haploid males via a sex pheromone. Mating takes place on the host plant, and females use their saw-like ovipositor to embed their full complement of eggs within the needles of a single pine branch. Larvae emerge and feed on pine needles before dispersing to the soil to spin a cocoon.

While N. pinetum and N. lecontei share many similarities, N. pinetum feeds exclusively on white pine (Pinus strobus) and N. lecontei tends to avoid this host. Differences between their hosts probably generate divergent selection on many different larval and adult traits (Bendall et al., 2017; Codella & Raffa, 2002; Coppel & Benjamin, 1965; Lindstedt et al., 2022). For example, differences in needle chemistry and thickness between the preferred hosts of N. lecontei and N. pinetum are associated with differences in egg size, female ovipositor morphology and female egg-laying behaviours. These traits, which together determine the reproductive success of adult females, act as an ecological barrier to gene exchange in sympatric populations (Bendall et al., 2017). This previous work suggests that many regions of the genome are likely to be under divergent selection between these species. Moreover, a coalescent-based analysis revealed evidence of historical mitochondrial introgression, suggesting that this species pair has diverged with gene flow (Linnen & Farrell, 2007).

We hypothesize that adaptation to different pines and speciation-with-gene-flow in *N. lecontei* and *N. pinetum* was facilitated by sex-limited hemizygosity and recombination. To evaluate this possibility, we: (i) simulate diploid and haplodiploid "genomes" (500-kb loci) evolving under mutation, drift, divergent selection, migration and recombination; (ii) model the divergence history and characterize patterns of genomic differentiation in sympatric populations of *N. lecontei* and *N. pinetum*; and (iii) use our estimated divergence history and other system-specific details to parameterize simulations of haplodiploid and diploid genomes evolving under varying levels of selection. Our data support a faster-haplodiploid effect in *Neodiprion* sawflies, and based on our results, we suggest that such effects may have promoted adaptation and speciation in haplodiploid taxa.

2 | METHODS

2.1 | Simulation of haplodiploid and diploid chromosomes under divergence-with-gene-flow

To evaluate the effects of hemizygous selection and sex-limited recombination on genomic differentiation patterns, we simulated populations of diploid autosomes and haplodiploid chromosomes (Figure 1). We used SLIM version 3 (Haller & Messer, 2019) to simulate 500- kb chromosomes evolving via mutation, drift, migration and selection, using X-chromosomes to mimic haplodiploids and autosomes to mimic diploids. We considered an isolation-with-migration model with two populations that diverged at some time ($t_{\rm div}$) from an ancestral population, with symmetric gene flow (Figure 1b). Simulations consisted of two phases. First, to enable the ancestral population to reach mutation-drift equilibrium, we simulated neutral evolution of an ancestral population with an effective size of 1,500 $(2N_s)$, a mutation rate of 2.5×10^{-7} per bp per generation, and a recombination rate of 2.5×10^{-7} per bp per generation for 10,000 generations (>4N_a generations). Second, to simulate divergence-with-gene-flow, the ancestral population splits into two equally sized populations (2N_e) that exchange migrants at a constant and symmetrical migration rate ($m = m_{12} = m_{21}$). The timing of this split coincides with the onset of divergent natural selection on a polymorphic site (initial frequency of derived allele a denoted as q_0) located at the middle of the chromosome (250 kb). We modelled selection under a "parallel dominance" fitness model in which the derived allele a is favoured in population 1 and allele A (ancestral allele) is favoured in population 2, its dominance is the same irrespective of the population—Figure 1a, as in Moran (1959) and Lasne et al., (2017). We chose this model to facilitate comparison with previous work (Lasne et al., 2017) and because this model is consistent with biochemical mechanisms underlying dominance (Curtsinger et al., 1994; Rosenblum et al., 2010). Furthermore, we assumed identical selection coefficients (s) and dominance (h) in diploids and haplodiploids, but because of direct selection in hemizygous males, the efficiency of selection might differ (Supporting Methods). Our model assumes there are separate sexes, with equal numbers of diploid males and diploid females (diploid case) or equal numbers of haploid males and diploid females (haplodiploid case). Our model also assumes equal migration rates, similar distributions of offspring numbers for males and females, and that the fitness of hemizygous males (A or a) is equal to the fitness of corresponding homozygous females (AA or aa). Following the onset of selection, populations evolve for an additional 2,000 generations.

To control for factors other than hemizygous selection and sex-limited recombination that might also cause differences in genomic differentiation between diploids and haplodiploids, our simulations were scaled so that haplodiploid and diploid chromosomes experience equivalent effective levels of drift (same effective size, N_e), migration (m) and recombination (r) (i.e., have identical scaled mutation rate [$\theta = 4N_e\mu L$], scaled recombination rate [$\rho = 4N_er L$] and scaled migration rate [$2N_em$]; Table S1). Thus, we adjusted the N_e to

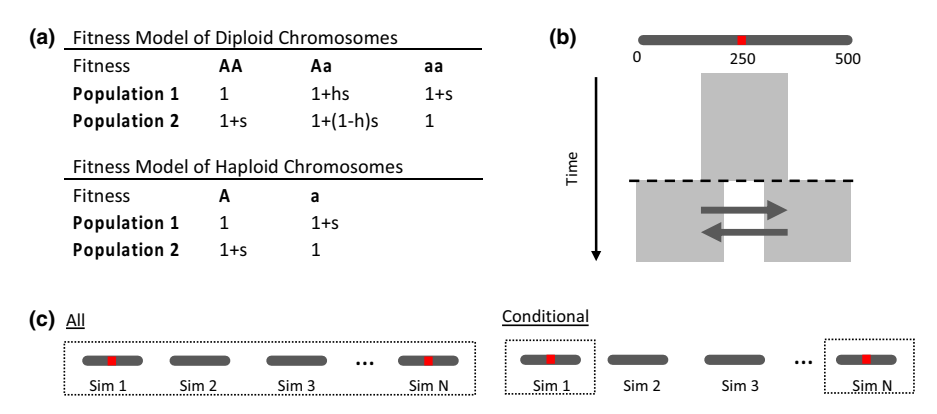


FIGURE 1 Overview of the simulation approach for evaluating faster-haplodiploid effects on genomic differentiation. (a) Fitness models for diploid chromosomes (diploid autosomes and haplodiploid females) and haploid chromosomes (haplodiploid males). This is a parallel dominance model in which the fitness of heterozygotes depends on the dominance of allele a, which is assumed to be the same in both populations. Population 1 is the population where the derived allele is beneficial. (b) Overview of stochastic simulations under an isolation-with-migration model. An ancestral population with an effective size of $2N_e$ =1,500 gene copies (i.e., a haplodiploid locus with 500 females and 500 males or a diploid locus with 375 females and 375 males) of a 500-kb chromosome (dark grey bar) evolves for 10,000 generations to reach mutation-drift equilibrium. This population then splits into two equally sized populations. A divergently selected site at position 250 kb (red line) with two alleles (A and a) is introduced at the time of split, with an initial frequency a0 of allele a1 in both populations. The populations evolve for a1 a2,000 generations, experiencing symmetric migration at a constant rate. For each parameter combination, 1,000 simulations were run. (c) Two approaches were used to summarize simulation results. In the "all"-simulations approach, mean a1 is computed only using simulations in which the derived allele a2 was lost due to drift). In the "conditional" approach, mean a3 is computed only using simulations for which the derived allele a3 was retained [Colour figure can be viewed at wileyonlinelibrary.com]

ensure that both the diploid and haplodiploid chromosomes have $2N_a = 1,500$, which is the N_a of a hemizygous locus with N = 1,000individuals (500 females with two copies and 500 males with one copy). This corresponds in the diploid case to $N_D = 750$ individuals, obtained as $N_D = xN$ individuals, where x is a scaling factor that is 3/4 for a 0.50 sex-ratio (Supporting Methods). Because a haplodiploid chromosome spends 2/3 of the time in the sex in which it recombines (Kong et al., 2002; Wilfert et al., 2007), to ensure identical average recombination rates in diploids and haplodiploids we scaled the SLIM diploid recombination rate as 2/3 of the recombination rate specified in SLIM for haplodiploids (because males do not recombine). To confirm our scaling, we verified that the values of several summary statistics measuring diversity, differentiation and linkage disequilibrium were identical for neutral simulations for haplodiploid and diploid chromosomes, and that they converged to the expected values under neutrality (Figure S1). The parameter values above are identical to a scaled mutation rate ($\theta = 4N_o \mu L$) and recombination rate ($\rho = 4N_o rL$) of a 500-kb chromosome in a population with an effective size of $2N_a = 100,000$ and a mutation rate of 2.5×10^{-9} per bp per generation. We used a smaller effective population size of 1,500 and scaled the other parameters accordingly to reduce the computational burden of forward simulations, as is usually done when using SLIM (e.g., Phung et al., 2016). Our chosen divergence time corresponds to a divergence with a scaled time $T_{div}/(4N_e) = 2/3$, which is within the range of values estimated for pairs of closely related populations and species across many taxa (Hey & Pinho, 2012; Pinho & Hey, 2010), but lower than the threshold of $T_{div}/(4N_e) > 1$ (and $2N_e m < 1$) proposed by Hey and Pinho (2012) as a diagnostic for fully independent species.

We simulated diverging populations under all possible combinations of seven selection coefficients (scaled $2N_e$ s ~0, 10, 20, 40,

80, 100, 200), four migration rates (scaled $2N_am \sim 0.0, 0.5, 2.5, 5.1$), two dominance coefficients (recessive h = 0.01 and codominant h = 0.50) and four different starting allele frequencies ($q_0 = 1/(2N_e)$, 0.01, 0.10, and 0.50; Table S1). These parameters were chosen to capture a range of selection coefficients and migration rates, including the neutral case (s = 0) and the no-migration case (m = 0). Our values of 2N_am were chosen such that they fell both below and above the threshold for divergence via drift $2N_{o}m = 1$ (Hey & Pinho, 2012). Our values of $2N_a s$ range from $10 \times$ the threshold for selection to be considered "nearly neutral" ($2N_{o}s = 1$) to $200 \times$ that threshold, corresponding to moderate to strong selection (Lasne et al., 2017). For the populations we modelled, these are equivalent to s = 0.007-0.133, which correspond well to empirical estimates of s from natural populations (Thurman & Barrett, 2016). The starting allele frequencies ranged from new $(q_0 = 1/(2N_e))$ or rare $(q_0 = 0.01)$ mutations to common variants ($q_0 = 0.10$ and 0.50). To investigate the impact of recombination rate on linked variation we repeated a subset of these conditions (with $q_0 = 0.10$ and 0.50) under a lower recombination rate ($r = 0.1\mu = 2.5 \times 10^{-8}$ per bp per generation). For each unique combination of parameters, we performed 1,000 simulations.

For each replicate, we followed the trajectories of allele frequencies at the selected site in both populations, which were used to compute the number of simulations that retained the derived allele a in population 1. To investigate patterns of variation in samples rather than at the population level, in the last generation we sampled 20 chromosomes of 500 kb from each population. For each parameter combination, we computed average nucleotide diversity, D_{xy} and weighted $F_{\rm ST}$ across simulations using the Hudson estimator (Bhatia et al., 2013), averaged across all single nucleotide polymorphisms (SNPs) at three scales: (i) a 20-kb window centred on the

selected site ("20-kb"), (ii) across the 500-kb chromosome ("500-kb") and (ii) scan of contiguous nonoverlapping 20-kb windows ("genome scan"). We used these two window sizes to investigate the effects of haplodiploidy on sites closely linked to the selected site and on a chromosomal level in a manner that would mimic an empirical data set used for genome-wide scans. To measure patterns of linkage disequilibrium, we computed average r^2 between all pairs of SNPs within 20-kb windows. To evaluate the effect of loss of the derived allele a, we used two approaches: in the "all simulations" approach, the mean of summary statistics (e.g., F_{ST}) was computed across all simulations, whereas in the "conditional" approach, the mean of summary statistics is computed only across simulations where the derived allele was retained in population 1 (Figure 1c). Thus, the "conditional" approach removes the effect of allele loss. Parameter combinations for which fewer than 10 simulations were retained were treated as missing data.

2.2 | Empirical data: Estimating divergence history in a haplodiploid species pair

2.2.1 | Population sampling

We sampled 23 Neodiprion pinetum larvae and 44 N. lecontei larvae from Kentucky (Table S2). Larvae tend to be found in gregarious colonies of siblings in both species. To ensure we were not sampling close relatives, each individual was collected from a different colony. To maximize our chances of sequencing diploid female larvae, which tend to be larger than haploid male larvae, we extracted DNA from large larvae and verified sex with heterozygosity estimates. To evaluate whether there is ongoing hybridization between these species, we also sampled three individuals from Kentucky with intermediate larval pigmentation (suspected hybrids) and one laboratory-reared female F_1 hybrid as a positive control (Table S2). An additional 18 N. lecontei samples from an allopatric population in Michigan (Table S2) and one N. virginiana from Blackstone, VA (37°06'47.2"N, 78°01'37.4"W) were sequenced for use in demographic analyses.

2.2.2 | DNA sequencing

We extracted DNA using a CTAB/phenol-chloroform-isoamyl alcohol method (Chen et al., 2010). We visualized the DNA on a 0.8% agarose gel to confirm quality. To quantify the DNA, we used a Quant-iT High-Sensitivity DNA Assay Kit (Invitrogen – Molecular Probes). For *N. pinetum*, *N. lecontei* and hybrids, we used a modified double digest (dd)RAD sequencing protocol from Bagley et al. (2017) and Peterson et al. (2012). We fragmented the DNA using *Nla*III and *Eco*RI. We assigned each individual along with additional samples from other projects to one of eight libraries. During adapter ligation, each sample was also assigned one of 48 unique in-line barcodes (Table S2). We used the 5- to 10-bp variable length barcodes

used in Burford Reiskind et al. (2016). We then pooled each group of samples and size selected for a 379-bp fragment (±76 bp) on a PippinPrep (Sage Science). We performed 12 rounds of high-fidelity PCR (polymerase chain reaction) amplification (Phusion High-Fidelity DNA Polymerase) using PCR primers that included one of 12 unique Illumina multiplex read indices (Table S2). To allow for the detection of PCR duplicates, we included a string of four degenerate bases next to the Illumina read index (Schweyen et al., 2014). We used a Bioanalyzer 2100 (Agilent) to check library quality. The libraries were sequenced at the University of Illinois Roy J. Carver Biotechnology Center, using two lanes of Illumina HiSeq 4000 and150-bp single-end reads.

For *N. virginiana*, which we used as an outgroup, we used 150 paired-end reads generated on an Illumina Nextseq at the Univeristy of Georgia Genomics Facility (Vertacnik, 2020). Library preparation and whole-genome shotgun sequencing were both completed at the sequencing facility. We removed the adapters using CUTADAPT 1.16 and contaminants using the standard and pine databases in KRAKEN (Martin, 2011; Wood & Salzberg, 2014).

2.2.3 | DNA processing and variant calling

We aligned demultiplexed ddRAD reads to the N. lecontei reference genome (Nlec1.1 GenBank assembly accession no. GCA_001263575.2; Linnen et al., 2018; Vertacnik & Linnen, 2015) using the very sensitive setting in BOWTIE2 (Langmead & Salzberg, 2012). We only retained reads that aligned to one locus in the reference genome and had a Phred score >30. For the ddRAD data set, we removed PCR duplicates using a custom script. We called SNPs in SAMTOOLS (Li et al., 2009). Male and female larvae are morphologically indistinguishable. To identify putative haploid males, which are expected to have unusually low heterozygosity, we computed perindividual heterozygosity (as in Bagley et al., 2017). No individuals were excluded based on heterozygosity. We required all sites to have a minimum of 7x coverage and 50% missing data or less. We also removed SNPs with significantly more heterozygotes than expected under Hardy-Weinberg equilibrium (an indicator of genotyping/mapping error). We removed any individual that was missing more than 70% of the data. We performed all filtering in VCFTOOLS version 0.1.13 (Danecek et al., 2011).

We created several data sets with subsets of individuals and additional filtering for each of the population genetic analyses. We generated three data sets with minor allele filtering (MAF, SNPs <0.01 removed): (i) sympatric N. pinetum and N. lecontei for genome-wide patterns of divergence (36,935 SNPs); (ii) sympatric N. pinetum, N. lecontei and hybrids for admixture analysis (35,649 SNPs); and (iii) sympatric N. pinetum, N. lecontei, allopatric N. lecontei and outgroup N. virginiana for ABBA-BABA tests (12,905 SNPs). We also generated a down-sampled data set (described below) without an MAF filter for estimating site-frequency spectra (SFS) that included sympatric N. pinetum, N. lecontei and N. virginiana for demographic analyses.

2.2.4 | Population structure, demographic analysis, and genomic differentiation

To confirm that our suspected hybrids were genetically admixed, we used ADMIXTURE version 1.3.0 (Alexander et al., 2009) to estimate the proportion of ancestry for each individual collected in Kentucky (N. lecontei, N. pinetum, laboratory-reared hybrids and suspected field-caught hybrids) from K populations for K=1-5. We ran 100 replicates per K and chose the K with the lowest cross-validation (CV) score (Table S3). Additionally, to test for introgression between sympatric N. lecontei (P1) and N. pinetum (P3), we performed an ABBABABA test (Patterson et al., 2012) with Kentucky N. lecontei (P1), Michigan N. lecontei (allopatric population, P2), Kentucky N. pinetum (P3) and N. virginiana (outgroup, P4). We used a custom R script to compute the ABBA-BABA assuming that the outgroup is not fixed for the ancestral allele (Patterson et al., 2012), assessing significance with block-jackknife resampling dividing data into 645 blocks of ~20 SNPs.

To evaluate the timing and magnitude of gene flow between N. lecontei and N. pinetum, we performed demographic modelling based on the SFS using the composite likelihood method implemented in FASTSIMCOAL2 version 2.6 (Excoffier et al., 2013). For this analysis, we used ddRAD data from sympatric populations of N. lecontei and N. pinetum filtered as described above, with additional filters applied to satisfy analysis assumptions. First, to minimize the impact of linked selection on demographic history estimates, we used the NCBI Neodiprion lecontei Annotation Release 100 (updated to GCA 001263575.2) to exclude SNPs that were in or within 1 kb of the start or end of a gene, thereby generating a set of putatively neutral markers. Furthermore, to reduce bias in the SFS, we applied more stringent depth-of-coverage filters, requiring a minimum depth of 10x and a maximum depth less than 2x the median depth of coverage per individual. To build the 2D-SFS without missing data, each scaffold was divided into nonoverlapping 50-kb blocks, and we kept only blocks where the median distance between SNPs was >2 bp. SNPs without missing data were obtained for each block by downsampling four and six females from N. pinetum and N. lecontei, respectively. This resulted in a downsampled data set with 9,994 SNPs. To polarize the ancestral/derived state of alleles and obtain the unfolded 2D-SFS we used data from N. virginiana. To obtain the number of invariant sites in the 2D-SFS we assumed that the proportion of SNPs removed because of extra filters was the same for invariant sites. Given a proportion of number of SNPs to number of invariant sites before extra filters of ~0.046, the number of invariant sites in the 2D-SFS after filters was set to 215,283.

We tested five alternative demographic scenarios: (i) divergence without gene flow, (ii) divergence with continuous bidirectional migration, (iii) divergence in isolation followed by a single bout of secondary contact (bidirectional gene flow), (iv) divergence with bidirectional migration that stops before divergence is complete, and (v) divergence in isolation followed by continuous secondary contact (bidirectional). All models except the model of continuous gene flow

had an equal number of parameters, so we compared their likelihoods directly. We ran each model 100 times starting from different parameter combinations, each run with 50 optimization cycles (-I50) and approximating the expected SFS with 100,000 coalescent simulations (-n100000). We selected the run with the highest likelihood to estimate parameter values.

To examine genome-wide patterns of genetic divergence, we computed $F_{\rm ST}$ and π in 100-kb nonoverlapping windows for *N. lecontei* and *N. pinetum* in vcftools on the nondownsampled data set. To identify regions of the genome that were more or less differentiated than expected under neutrality, we simulated 10,000 data sets under the inferred demographic history for sawflies using coalescent simulations implemented in the R package *scrm* (Staab et al., 2015). For each simulation, we computed $F_{\rm ST}$ as for the *Neodiprion* data set (see above). Outlier windows were defined as those above or below the 95% confidence interval (CI) for $F_{\rm ST}$ obtained from the 10,000 simulations. Simulations were done assuming no recombination, 50% missing data (i.e., female sample sizes of 0.5 × 23 for *N. pinetum* and 0.5 × 44 for *N. lecontei*), and scaling theta ($4N\mu$) such that the average number of SNPs per window across simulations was similar to that observed in *Neodiprion* data set.

2.3 | Comparison of empirical haplodiploid data to simulated diploids and haplodiploids

To evaluate the potential influence of haplodiploidy on genomic differentiation between *N. lecontei* and *N. pinetum*, we used SLIM version 3 to simulate haplodiploid and diploid "genomes" evolving under divergent selection and the demographic history estimated for our focal species pair. Because *N. pinetum* is on the derived host plant (Linnen & Farrell, 2010), we modelled *N. pinetum* as population 1 (where derived allele *a* is favoured) and *N. lecontei* as population 2. For these simulations, we also assumed a sex ratio of 70 females to 30 males based on previously published sex ratios for *N. lecontei* and *N. pinetum* (Craig & Mopper, 1993; Harper et al., 2016). As in our first set of simulations, we scaled our simulations to ensure equivalent levels of drift, migration, mutation rates and recombination between diploids and haplodiploids.

To reduce the computational burden of forward SLIM simulations, we rescaled parameters such that under neutrality, the SFS obtained with SLIM was identical to the expected SFS obtained under the demographic history inferred with FASTSIMCOAL 2. This was achieved by ensuring that the scaled mutation rate $4N_{\rm A}\mu L$ for L sites was identical in both cases, where $N_{\rm A}$ is the ancestral effective size and μ is the mutation rate per site per generation. By considering a mutation rate two orders of magnitude higher ($\mu = 3.50 \times 10^{-7}$ rather than the 3.50×10^{-9} per bp per generation used for SFS-based inference) and that $L = 5 \times 10^5$ sites in SLIM corresponds to $L = 5 \times 10^4$ sites in the 2D-SFS used for FASTSIMCOAL 2 (including SNPs and invariant sites), the haploid effective population sizes were three orders of magnitude lower (328 for N. pinetum, 1,093

for N. lecontei and 1,982 for the ancestral population) and migration rates three orders of magnitude higher (3.64 \times 10⁻⁴ into N. pinetum, 1.71×10^{-5} into N. lecontei). The times of split were scaled accordingly, resulting in 1,548 generations (rather than 1.54×10^6). To obtain the number of individuals N in SLIM that correspond to the above haploid effective sizes, we had to account for the sex ratio of 70 females to 30 males (Supporting Methods). Given the average of 19.02 SNPs in Neodiprion 100-kb windows (with gaps due to sparse ddRAD loci), the average number of SNPs in SLIM simulations under neutrality of 2.257 would correspond to ~10 Mb of a similar ddRAD data set. We considered the recombination rate r to be three times higher than the mutation rate ($r = 1.05 \times 10^{-6}$) using an estimate of 3.43 centimorgans (cM) Mb⁻¹ based on a linkage map for N. lecontei constructed from an interpopulation cross (Linnen et al., 2018). To ensure the same average recombination rate for diploids and haplodiploids, the rate given as input in SLIM for diploids was scaled by 2/3 as done for the simulation study (see above). Because the perlocus selection estimate is unknown, we simulated differentiation and under a wide range of selection coefficients s from 0.0 to 0.3. We also simulated all combinations of two dominance coefficients (h = 0.01 and 0.50) and one starting allele frequency ($q_0 = 0.10$; Table S4). We computed mean $F_{\rm ST}$ across all 1,000 simulations for each starting allele frequency, dominance and selection coefficient combination. These combined simulations can be thought of as a divergence history in which, on average, there is a divergently selected site every 10 Mb.

3 | RESULTS

3.1 | Faster-haplodiploid effects on genomic differentiation with migration

Across all parameter combinations and for both window sizes (20and 500-kb), we found that $F_{\rm ST}$ between haplodiploid populations was always equal to or greater than $F_{\rm ST}$ between diploid populations (Figure 2). Migration and selection were both required for haplodiploid F_{ST} to exceed diploid F_{ST} , and the ratio of haplodiploid F_{ST} to diploid F_{ST} was close to 1 for many regions of parameter space. For both window sizes, we found that faster-haplodiploid effects (i.e., ratio of haplodiploid F_{ST} to diploid F_{ST} >1) were more pronounced in the recessive case (Figure 2a-d) than in the codominant case (Figure 2eh). For each dominance coefficient, the regions of parameter space that maximized faster-haplodiploid effects depended on the window size used to calculate F_{ST} . For sites tightly linked to the selected site (20-kb window), faster-haplodiploid effects were maximized when migration was high $(2N_{e}m \ge 2.5)$ and selection was moderate $(10 \le 2N_c s \le 40$; Figure 2b,f). By contrast, when we considered much larger 500-kb windows, relative differences between haplodiploid and diploid differentiation levels were maximized at higher selection coefficients (2N_s \geq 40) but at similar migration rates (2N_s \geq 2.5). The same trend-faster-haplodiploid effects maximized at higher selective coefficients for the 500-kb windows than for the 20-kb windows—was found for all initial frequencies of the derived allele

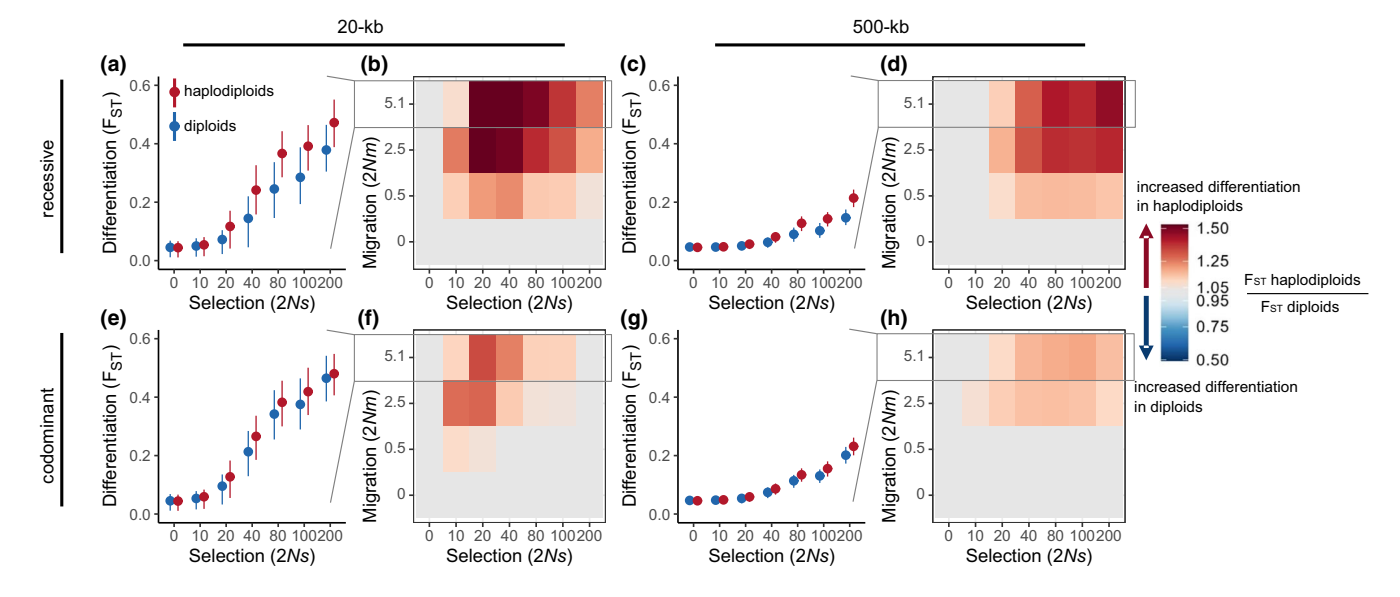


FIGURE 2 Faster-haplodiploid effects as a function of strength of divergent selection, migration rate and dominance. (a, e, c, g) Differentiation (F_{ST}) for haplodiploids and diploids with scaled migration rate 2Nm = 5.1 and varying scaled selective coefficients (2Ns) for different window sizes with selected site in the middle [(a, e) 20-kb, (c, g) 500-kb], and different dominance coefficients [(a, c) recessive (h = 0.01) and (e, g) codominant (h = 0.50)]. The points correspond to mean F_{ST} and the whiskers to the interquartile range based on 1,000 simulations. (b, d, f, h) Heatmap of the ratio of haplodiploid to diploid (H/D) mean F_{ST} for different combinations of selective coefficients and migration rates for different window sizes [(b, f) 20-kb and (d, h) 500-kb], and dominance coefficients [(b, d) recessive (h = 0.01) and (f, h) codominant (h = 0.50)]. Results were obtained with 1,000 simulations for each parameter combination with an initial frequency $q_0 = 0.10$, sampling 20 females from each population. The grey boxes and lines indicate the correspondence of mean differentiation values shown in (a, c, e, g) to heatmap F_{ST} ratios shown in (b, d, f, h). For heatmaps of the ratio of F_{ST} we considered that values between 0.95 and 1.05 to be 1.00 (i.e., no difference between haplodiploids and diploids) [Colour figure can be viewed at wileyonlinelibrary.com]

.16410 by Nationwide Children Hospital, Wiley Online Library on [01/03/2023]. See the Terms

ns) on Wiley Online Library for rules of use; OA articles are governed by the applicable Creative Commons

365294x, 2022, 8, Downloaded from https://onlinelibrary.wiley.com/doi/10.1111/mec.

a for the codominant case and for $q_0=0.5$ for the recessive case (Figure S2). However, for new ($q_0=1/(2N)$) or rare ($q_0=0.01$) recessive alleles, faster-haplodiploid effects were always maximized at the highest selection coefficients, regardless of window size (Figure S2).

One mechanism leading to greater differentiation in haplodiploids was differential allele retention. Simulations of haplodiploid populations had a higher probability of retaining the derived allele across a wide range of parameter combinations (Figure 3; Figure S3). For recessive alleles, differences in allele retention between haplodiploids and diploids were dependent on both starting allele frequency and selection strength, but were relatively insensitive to migration rate (Figure 3a; Figure S3). By contrast, except for a slightly elevated probability of retaining the derived allele at lower selection coefficients ($10 \le 2N_e s \le 20$, inset panel in Figure 3b), differences in allele retention between haplodiploid and diploid populations were minimal for the codominant case (Figure 3b). For both recessive and codominant cases, increasing migration had a limited but consistent effect, leading to a lower probability of allele retention.

To investigate the impact of haplodiploidy on genomic differentiation via mechanisms other than differential allele retention, we computed average F_{ST} for each parameter combination conditional on retaining the derived allele at the selected locus. For the recessive case, controlling for the impact of differential allele retention decreased the magnitude of faster-haplodiploid effects across all parameter combinations (Figure 4a vs. 2b and Figure 4e vs. 2d), indicating that the increased retention of the derived allele in haplodiploids contributed to faster-haplodiploid effects. Compared to the recessive case, conditioning on allele retention had much less of an impact on the magnitude of faster-haplodiploid effects for the codominant case (Table S5). The heatmaps in Figure 5(a,e) are nearly identical to those in Figure 2(f, h), respectively. This is unsurprising since differences in allele retention were minimal in the codominant case (Figure 3). Once we conditioned on retaining the derived allele, starting allele frequency had little impact on patterns of fasterhaplodiploid evolution (Figure S4; for comparison see Figure S2). Finally, as expected, decreasing the recombination rate increased the magnitude of faster-haplodiploid effects on linked variation (Figure S5).

The observation that haplodiploid $F_{\rm ST}$ tends to exceed diploid $F_{\rm ST}$ even after conditioning on retaining the derived allele (Figures 4a,b,e,f and 5a,b,e,f) indicates that mechanisms other than differential allele retention contribute to elevated differentiation in haplodiploids. To explore these mechanisms, we examined allele trajectories (Figures 4c,d and 5c,d) and chromosome-wide $F_{\rm ST}$ patterns (Figures 4g,h and 5g,h) under high migration (2Nm = 5.1) and two selection intensities (moderate: 2Ns = 40 and strong: 2Ns = 200). These plots revealed two sources of faster-haplodiploid effects in addition to differential allele retention (see Supporting Results for additional explanation of these mechanisms). First, during the initial stages of divergence, haplodiploids reached migration–selection equilibrium faster than diploids: $\sim 3\times$ faster for the recessive case (Figure 4c,d) and $\sim 1.2\times$ faster for the codominant case (Figure 5c,d).

The faster time to equilibrium in the codominant, strong-selection case resulted in a chromosome-wide faster-haplodiploid effect even though there was no difference in $F_{\rm ST}$ at the selected site (Figure 5h). Second, once migration–selection equilibrium was reached, haplodiploids tended to be more efficient than diploids at eliminating maladapted immigrant alleles in one or both populations (Figures 4c,d and 5c), resulting in elevated differentiation at sites tightly linked to the selected site (Figures 4g,h and 5g). Under strong selection and codominance, however, both haplodiploids and diploids were efficient at removing maladapted immigrant alleles from both populations (Figure 5d), resulting in similar differentiation levels at the selected site (Figure 5h).

Overall, our simulations suggest so long as there is migration, haplodiploidy will lead to elevated differentiation at selected sites and linked neutral sites when populations diverge via divergent selection. This "faster-haplodiploid effect" is produced under a wide range of selection coefficients, regardless of whether selection acts on new mutations, rare standing genetic variation or common standing genetic variation, and regardless of whether selection acts on recessive or codominant alleles (Figure 2; Figure S2). Finally, while the effects of hemizygous selection and sex-limited recombination tend to be most pronounced at selected sites and tightly linked neutral sites (20-kb windows), faster-haplodiploid effects can extend far beyond the selected site (500-kb windows, which translates to ~4.4 cM in our simulations).

3.2 | Demography and genomic differentiation in pine sawflies

Neodiprion lecontei and N. pinetum differ in many host-related traits (Figure 6a). Our admixture analysis of N. lecontei, N. pinetum, a laboratory-reared F_1 hybrid and three suspected wild-caught hybrids supported two distinct genetic clusters (K = 2; Table S3). Putative wild hybrids were indistinguishable from the laboratoryreared hybrid, and all four individuals were genetically admixed with approximately equal contributions from N. pinetum and N. lecontei (Figure 6b). The only other admixed individual detected was morphologically indistinguishable from N. pinetum, but an estimated ~13% of its genome came from N. lecontei. In addition to finding evidence of recent admixture, an ABBA-BABA test revealed evidence of historical introgression between sympatric N. pinetum and N. lecontei populations (D = 0.18; $p = 2.12 \times 10^{-15}$). Finally, demographic models that had no migration or only a single burst of admixture were far less likely than models that included continuous migration (Table 1). Together, these results support a divergence-with-geneflow scenario for N. lecontei and N. pinetum (Figure 6c).

Comparing three different models that included migration (starting after divergence, stopping before the present day or continuous migration), our SFS data were probably under the model that had the fewest parameters: a continuous migration model (Table 1). Maximum-likelihood parameter estimates under this model suggest that N. pinetum and N. lecontei diverged ~1.5 \times 10⁶ generations ago.

FIGURE 3 Effect of haplodiploidy on retaining the derived allele at the site under divergent selection. Probability of retaining—Prob(retention)—the derived allele a for haplodiploid and diploid simulations at the two extremes of migration rates considered: no migration (2Nm = 0; solid lines) and high migration (2Nm = 5.1, dotted lines), for (a) recessive (h = 0.01), and (b) codominant (h = 0.50) mutations. In (b), the inset shows a zoom for 2Ns values between 0 and 40. The probability of allele retention is calculated as the proportion of 1,000 simulations that retained the derived allele a in population 1 (where a is favoured). The 95% confidence intervals are Clopper–Pearson CI for proportions. These results are for an initial allele frequency of 0.10 ($a_0 = 0.10$) [Colour figure can be viewed at wileyonlinelibrary.com]

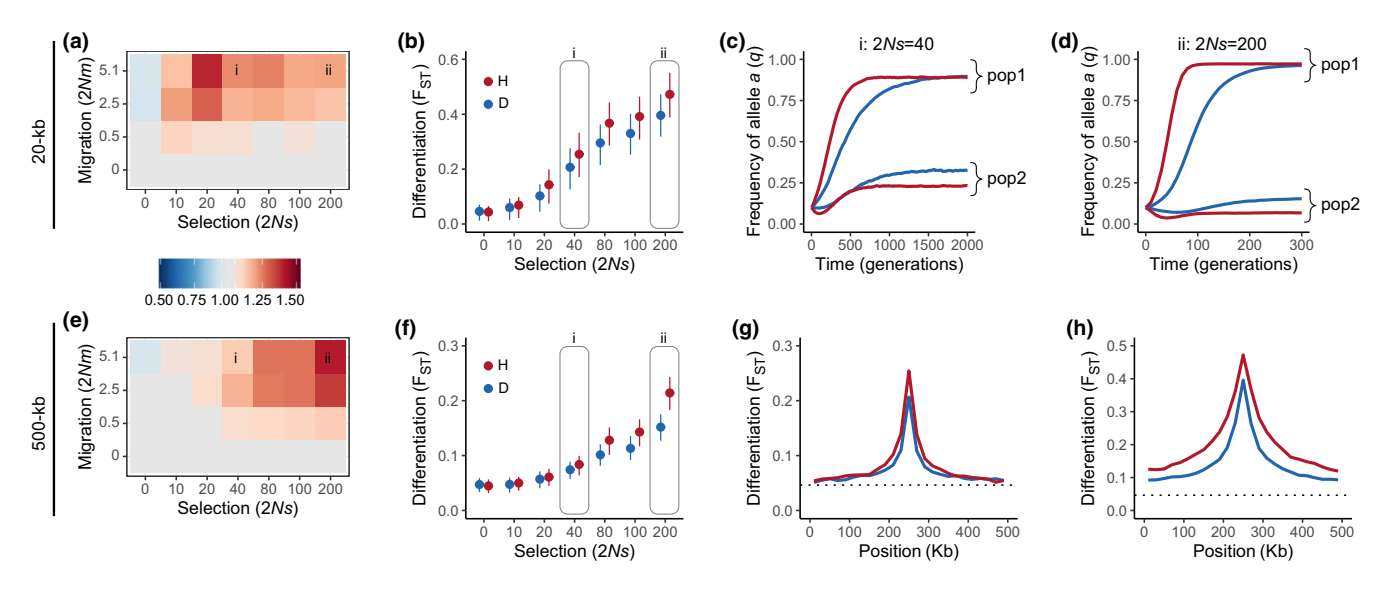
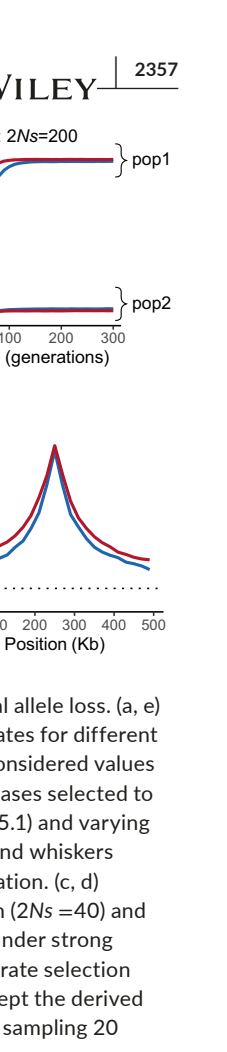


FIGURE 4 Faster-haplodiploid effects for a recessive (h = 0.01) derived allele after removing the effect of differential allele loss. (a, e) Heatmap of the ratio of haplodiploid (H) to diploid (D) mean F_{ST} for a combination of selective coefficients and migration rates for different window sizes with the selected site at the middle: (a) 20-kb and (e) 500-kb windows. For heatmaps of the ratio of F_{ST} we considered values between 0.95 and 1.05 to be 1.00 (i.e., no difference between haplodiploids and diploids). Labels i and ii indicate the two cases selected to illustrate allele trajectories and scans of differentiation. (b, f) F_{ST} for haplodiploids and diploids with high migration (2Nm = 5.1) and varying selective coefficients (2Ns), for different window sizes: (b) 20-kb and (f) 500-kb windows. Points correspond to mean F_{ST} and whiskers to interquartile ranges. Labels i and ii indicate the two cases selected to illustrate allele trajectories and scans of differentiation. (c, d) Trajectories of allele frequencies at the site under divergent selection in both populations, for: (c) moderate selection (2Ns = 40) and (d) strong selection (2Ns = 200). Note that the time scale is different because equilibrium differentiation is reached faster under strong selection. (g, h) Scan of mean F_{ST} along the 500-kb chromosome in nonoverlapping 20-kb windows, obtained for: (g) moderate selection (2Ns = 40) and (h) strong selection (2Ns = 200). Mean and interquartile F_{ST} are based on the simulations out of 1,000 that kept the derived allele a in population 1 at the site under divergent selection. Results are for simulations with an initial frequency $q_0 = 0.10$, sampling 20 females from each population [Colour figure can be viewed at wileyonlinelibrary.com]

Assuming one to three generations per year for KY populations of these species (Benjamin, 1955; Rauf & Benjamin, 1980; CL, personal observation), this estimate suggests that N. pinetum and N. lecontei probably diverged between 0.5 and 1.5 million years ago. Our parameter estimates also suggest that N. pinetum has a smaller N_e than N. lecontei, and that migration rates have been asymmetric,

with more migration from *N. lecontei* to *N. pinetum* than the reverse (Figure 6c, Table 1). Importantly, this model provides a good fit to the observed SFS and other summary statistics (Figure S6).

Despite continuous migration throughout divergence, genomewide average F_{ST} was high (F_{ST} =0.63). However, differentiation levels varied widely across the genome, with localized regions of both



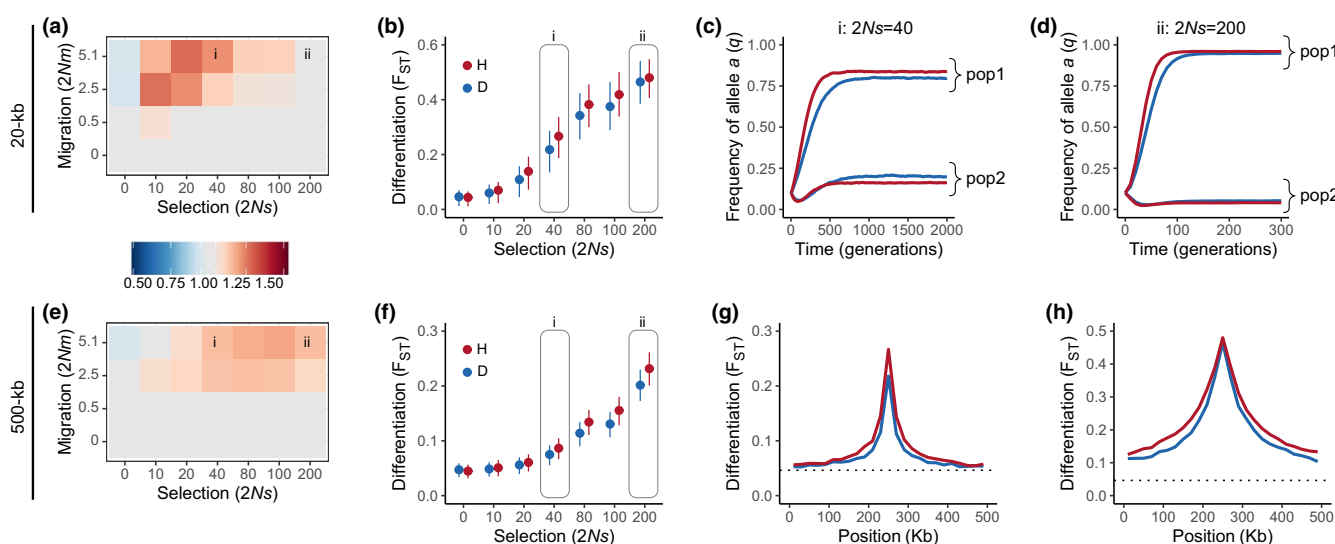


FIGURE 5 Faster-haplodiploid effects for a codominant (h = 0.50) derived allele after removing the effect of differential allele loss. (a, e) Heatmap of the ratio of haplodiploid (H) to diploid (D) mean F_{ST} for a combination of selective coefficients and migration rates for different window sizes with the selected site at the middle: (a) 20-kb and (e) 500-kb windows. For heatmaps of the ratio of F_{ST} we considered values between 0.95 and 1.05 to be 1.00 (i.e., no difference between haplodiploids and diploids). Labels i and ii indicate the two cases selected to illustrate allele trajectories and scans of differentiation. (b, f) F_{ST} for haplodiploids and diploids with high migration (2Nm = 5.1) and varying selective coefficients (2Ns), for different window sizes: (b) 20-kb and (f) 500-kb windows. Points correspond to mean F_{ST} and whiskers to interquartile ranges. Labels i and ii indicate the two cases selected to illustrate allele trajectories and scans of differentiation. (c, d) Trajectories of mean allele frequencies at the site under divergent selection in both populations, for: (c) moderate selection (2Ns = 40) and (d) strong selection (2Ns = 200). Note that the time scale is different because equilibrium differentiation is reached faster under strong selection. (g, h) Scan of mean F_{ST} along the 500-kb chromosome in nonoverlapping 20-kb windows, obtained for: (g) moderate selection (2Ns = 40) and (h) strong selection (2Ns = 200). Mean and interquartile F_{ST} are based on the simulations out of 1,000 that kept the derived allele a in population 1 at the site under divergent selection. Results are for simulations with an initial frequency $q_0 = 0.10$, sampling 20 females from each population [Colour figure can be viewed at wileyonlinelibrary.com]

very high and very low F_{ST} (Figure 7). Using simulations according to the inferred demographic history to generate 95% confidence intervals for F_{ST} under neutrality revealed evidence of both high- F_{ST} and low- F_{ST} outliers in our empirical data set (Figure 7). These regions are candidates for divergent selection and adaptive introgression, respectively. Nucleotide diversity (π) for both N. pinetum and N. lecontei also varied across the genome, but N. lecontei had a higher average π (2.71 \times 10⁻⁵) than N. pinetum (1.95 \times 10⁻⁵), which is consistent with the differences in effective population size between the two species (Table 1). Overall, demographic modelling and genomic differentiation patterns are consistent with the hypothesis that this species pair diverged with substantial gene flow, while experiencing divergent selection at many unlinked locations throughout the genome.

3.3 | Expectations for faster-haplodiploid effects under inferred demographic model

There were several differences between our simulations and our empirical system, including lower migration rates and asymmetries in both effective population size and migration rate (Table 1) as well as female-biased sex ratios (Harper et al., 2016). To capture some of these system-specific characteristics, we simulated haplodiploid and

diploid populations evolving under the demographic model we estimated from our sawfly data. A comparison between our observed summary statistics (SFS, F_{ST} , Π , D_{xy} and r^2) for the putatively neutral intergenic regions and summary statistics obtained from neutral simulations (2Ns =0) shows that the demographic model implemented in SLIM is working as expected, and that our simulated diploid and haplodiploid chromosomes do not differ under neutrality (Figure S6).

When we included divergent natural selection in our sawfly-parameterized simulations of diploid and haplodiploid genomes, we again observed faster-haplodiploid effects on the "genome-wide" mean $F_{\rm ST}$ for both dominant and recessive alleles under a range of selection coefficients (Figure 8). As observed for simulations under the simpler isolation-with-migration model, the magnitude of this effect was highest for recessive alleles and moderate-to-strong selection. These simulations also demonstrate that faster-haplodiploid effects can be observed with female-biased sex ratios and with asymmetric migration.

4 | DISCUSSION

Haplodiploid taxa are numerous and ecologically diverse (Forbes et al., 2018; Hölldobler & Wilson, 1990). While haplodiploid diversity

(a)

lecontei ż

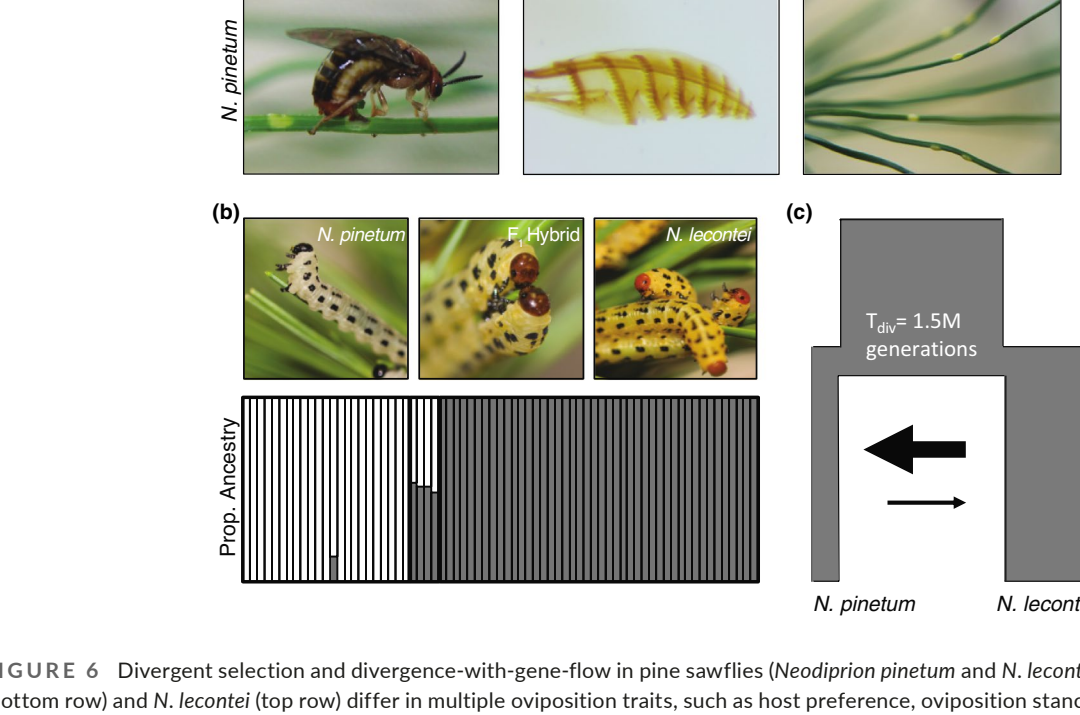


FIGURE 6 Divergent selection and divergence-with-gene-flow in pine sawflies (Neodiprion pinetum and N. lecontei). (a) N. pinetum (bottom row) and N. lecontei (top row) differ in multiple oviposition traits, such as host preference, oviposition stance (first column), ovipositor morphology (second column), and spacing and number of eggs per needle (last column), resulting in strong extrinsic postzygotic isolation. These oviposition traits along with additional host-use adaptations probably result in multiple independent regions of the genome experiencing divergent selection. (b) Representative images of N. pinetum, N. lecontei and F_4 hybrid larvae above an ADMIXTURE plot (K=2) of individuals sampled from Kentucky. N. pinetum ancestry is in white; N. lecontei ancestry is in grey. Laboratory-reared (N = 1) and field-caught (N = 3) hybrids are genetically admixed with approximately half of their ancestry coming from each species. (c) N. pinetum and N. lecontei have diverged with continuous but asymmetric gene flow. The diagram is based on an estimated demographic model for this species pair, with width of boxes proportional to population size and width of arrows proportional to migration rate (see Table 1) [Colour figure can be viewed at wileyonlinelibrary.com]

could be due to low transition rates between haplodiploidy and diploidy, it is also possible that haplodiploidy increases speciation rates (Blackmon et al., 2017; Koevoets & Beukeboom, 2008; Lohse & Ross, 2015; Patten et al., 2015). Here we explore one avenue through which haplodiploidy may facilitate speciation: by increasing genomic differentiation and linkage disequilibrium between populations that diverge with gene flow. Specifically, our simulations reveal that with both selection and migration, haplodiploid populations will maintain higher levels of differentiation than comparable diploid populations. This is true not only at the selected site, but also up to ~20 cM away. With the sawfly empirical data, we identify a potential case of sympatric divergence via adaptation to different hosts. Here, we discuss implications of these results for faster-X theory, evolution in haplodiploids and models of sympatric speciation. We also discuss some limitations of our models and data and highlight priorities for future work.

Faster-haplodiploid effects under divergencewith-gene-flow and relevance to faster-X theory

Overall, our simulations demonstrate multiple mechanisms through which genomic differentiation in haplodiploids is increased relative to diploids when populations diverge with gene flow. Given similarities between the transmission genetics of haplodiploid genomes and X chromosomes, these findings are also relevant to faster-X theory. As described below, our simulations recapitulate several key results from previous work on faster-X theory, albeit in some additional corners of parameter space (e.g., divergencewith-gene-flow via new or rare mutations; cf. Lasne et al., 2017). Based on our simulations, we can group faster-haplodiploid effects and mechanisms into three distinct phases. In the first phase, the dynamics of a divergently selected, low-frequency allele is mostly determined by the risk of loss due to drift (Figure 3; Figure

TABLE 1 Maximum-likelihood values and maximum-likelihood parameter estimates for the five demographic models tested

Parameters migration migration divergence present day migration No. of parameters estimated 7 7 7 7 6 Ancestral population size 2075281 1962052 1971660 2006404 1982187 N. pinetum population size 645779 369032 322897 337579 328311 N. lecontei population size 1057278 1052921 1104528 1075336 1093739 Time since divergence (generations) 1010864 1255392 1542789 1553120 1548690 N. pinetum bottleneck size 717 NA NA NA NA N. pinetum bottleneck size 470 NA NA NA NA N. lecontei bottleneck size 470 NA NA NA NA Admixture proportion from N. pinetum to N. lecontei NA 0.0060941 NA NA NA Admixture proportion from N. lecontei to N. pinetum NA 0.118292 NA NA NA Migration rate from N. lecontei to N. pin					•	
Ancestral population size 2075281 1962052 1971660 2006404 1982187 N. pinetum population size 645779 369032 322897 337579 328311 N. lecontei population size 1057278 1052921 1104528 1075336 1093739 Time since divergence (generations) 1010864 1255392 1542789 1553120 1548690 N. pinetum bottleneck size 717 NA NA NA NA NA N. lecontei bottleneck size 470 NA NA NA NA NA Time since bottleneck 1010854 NA NA NA NA NA Admixture proportion from N. pinetum to N. lecontei NA 0.0060941 NA NA NA NA Admixture proportion from N. lecontei to N. pinetum NA 0.118292 NA NA NA Migration rate from N. lecontei to N. pinetum NA NA NA NA NA Migration rate from N. lecontei to N. pinetum NA NA NA NA NA NA NA Migration rate from N. pinetum to N. lecontei NA	Parameters		contact with one burst of	migration that starts after	migration that ends before	Continuous migration
N. pinetum population size 645779 369032 322897 337579 328311 N. lecontei population size 1057278 1052921 1104528 1075336 1093739 Time since divergence (generations) 1010864 1255392 1542789 1553120 1548690 N. pinetum bottleneck size 717 NA NA NA NA NA N. lecontei bottleneck size 470 NA NA NA NA NA Time since bottleneck 1010854 NA NA NA NA NA Admixture proportion from N. pinetum to N. lecontei NA 0.0060941 NA NA NA Admixture proportion from N. lecontei to N. pinetum NA 0.118292 NA NA NA Migration rate from N. lecontei to N. pinetum NA 115046 NA NA NA Mumber of N. pinetum to N. lecontei NA NA NA 1.64E-08 1.83E-08 1.71E-08 Number of N. pinetum migrants NA NA NA 0.018665 </td <td>No. of parameters estimated</td> <td>7</td> <td>7</td> <td>7</td> <td>7</td> <td>6</td>	No. of parameters estimated	7	7	7	7	6
N. lecontei population size 1057278 1052921 1104528 1075336 1093739 Time since divergence (generations) 1010864 1255392 1542789 1553120 1548690 N. pinetum bottleneck size 717 NA NA NA NA N. lecontei bottleneck size 470 NA NA NA NA Time since bottleneck 1010854 NA NA NA NA Admixture proportion from N. pinetum to N. lecontei NA 0.0060941 NA NA NA Admixture proportion from N. lecontei to N. pinetum NA 0.118292 NA NA NA Time since admixture NA 115046 NA NA NA Migration rate from N. lecontei to N. pinetum NA NA 3.94E-07 3.63E-07 3.65E-07 Migration rate from N. pinetum to N. lecontei NA NA NA 1.83E-08 1.71E-08 Number of N. pinetum migrants NA NA NA 0.018665 0.018665 Number of N. lecontei m	Ancestral population size	2075281	1962052	1971660	2006404	1982187
Time since divergence (generations) 1010864 1255392 1542789 1553120 1548690 N. pinetum bottleneck size 717 NA NA NA NA NA N. lecontei bottleneck size 470 NA NA NA NA NA Time since bottleneck 1010854 NA NA NA NA NA Admixture proportion from N. pinetum to N. lecontei NA 0.0060941 NA NA NA Admixture proportion from N. lecontei to N. pinetum NA 0.118292 NA NA NA Admixture proportion from N. lecontei to N. pinetum NA 0.118292 NA NA NA Migration rate from N. lecontei to N. pinetum NA NA NA NA NA Migration rate from N. lecontei to N. pinetum NA NA NA 1.64E-08 1.83E-03 1.71E-08 Number of N. pinetum migrants NA NA NA 0.018423 0.0196645 0.018665 Time since migration started NA NA <t< td=""><td>N. pinetum population size</td><td>645779</td><td>369032</td><td>322897</td><td>337579</td><td>328311</td></t<>	N. pinetum population size	645779	369032	322897	337579	328311
N. pinetum bottleneck size 717 NA NA NA NA N. lecontei bottleneck size 470 NA NA NA NA Time since bottleneck 1010854 NA NA NA NA Admixture proportion from N. pinetum to N. lecontei NA 0.0060941 NA NA NA Admixture proportion from N. lecontei to N. pinetum NA 0.118292 NA NA NA Admixture proportion from N. lecontei to N. pinetum NA 0.118292 NA NA NA Migration rate from N. lecontei to N. pinetum NA 115046 NA NA NA Migration rate from N. lecontei to N. pinetum NA NA NA 1.64E-08 1.83E-08 1.71E-08 Number of N. pinetum migrants NA NA NA 0.1226254 0.119698 Number of N. lecontei migrants NA NA NA 0.018665 0.018665 Time since migration started NA NA NA NA NA Time since migratio	N. lecontei population size	1057278	1052921	1104528	1075336	1093739
N. lecontei bottleneck size 470 NA <	Time since divergence (generations)	1010864	1255392	1542789	1553120	1548690
Time since bottleneck 1010854 NA NA NA NA Admixture proportion from N. pinetum to N. lecontei NA 0.0060941 NA NA NA Admixture proportion from N. lecontei to N. pinetum NA 0.118292 NA NA NA Time since admixture NA 115046 NA NA NA Migration rate from N. lecontei to N. pinetum NA NA 3.94E-07 3.63E-07 3.65E-07 Migration rate from N. pinetum to N. lecontei NA NA 1.64E-08 1.83E-08 1.71E-08 Number of N. pinetum migrants NA NA 0.1273259 0.1226254 0.119698-0.19698-0.19669 Number of N. lecontei migrants NA NA NA 0.0181423 0.0196645 0.018665 Time since migration started NA NA NA NA NA Time since migration ended NA NA NA NA NA NA Estimated maximum likelihood (log 10) -32034.2 -32805.5 -32794.6 -32795	N. pinetum bottleneck size	717	NA	NA	NA	NA
Admixture proportion from N. pinetum to N. lecontei NA 0.0060941 NA NA NA Admixture proportion from N. lecontei to N. pinetum NA 0.118292 NA NA NA Time since admixture NA 115046 NA NA NA Migration rate from N. lecontei to N. pinetum NA NA 3.94E-07 3.63E-07 3.65E-07 Migration rate from N. pinetum to N. lecontei NA NA 1.64E-08 1.83E-08 1.71E-08 Number of N. pinetum migrants NA NA 0.1273259 0.1226254 0.1196984 Number of N. lecontei migrants NA NA NA 0.0181423 0.0196645 0.018665 Time since migration started NA NA NA 901891 NA NA Time since migration ended NA NA NA NA NA NA Estimated maximum likelihood (log 10) -33034.2 -32805.5 -32794.6 -32795 -32727.9 Maximum observed likelihood (log 10) -32727.9 -32727.9 <td< td=""><td>N. lecontei bottleneck size</td><td>470</td><td>NA</td><td>NA</td><td>NA</td><td>NA</td></td<>	N. lecontei bottleneck size	470	NA	NA	NA	NA
Admixture proportion from N. lecontei to N. pinetum NA 0.118292 NA NA NA Time since admixture NA 115046 NA NA NA Migration rate from N. lecontei to N. pinetum NA NA 3.94E-07 3.63E-07 3.65E-07 Migration rate from N. pinetum to N. lecontei NA NA 1.64E-08 1.83E-08 1.71E-08 Number of N. pinetum migrants NA NA 0.1273259 0.1226254 0.119698-0.019698-0.0196645 Number of N. lecontei migrants NA NA 0.0181423 0.0196645 0.018665 Time since migration started NA NA 901891 NA NA Time since migration ended NA NA NA 1906 NA Estimated maximum likelihood (log 10) -33034.2 -32805.5 -32794.6 -32795 -32794.3 Maximum observed likelihood (log 10) -32727.9 -32727.9 -32727.9 -32727.9 -32727.9	Time since bottleneck	1010854	NA	NA	NA	NA
Time since admixture NA 115046 NA NA NA Migration rate from N. lecontei to N. pinetum NA NA 3.94E-07 3.63E-07 3.65E-07 Migration rate from N. pinetum to N. lecontei NA NA 1.64E-08 1.83E-08 1.71E-08 Number of N. pinetum migrants NA NA 0.1273259 0.1226254 0.119698-0.01 Number of N. lecontei migrants NA NA 0.0181423 0.0196645 0.018665 Time since migration started NA NA 901891 NA NA Time since migration ended NA NA NA 1906 NA Estimated maximum likelihood (log 10) -33034.2 -32805.5 -32794.6 -32795 -32794.3 Maximum observed likelihood (log 10) -32727.9 -32727.9 -32727.9 -32727.9 -32727.9	Admixture proportion from N. pinetum to N. lecontei	NA	0.0060941	NA	NA	NA
Migration rate from N. lecontei to N. pinetum NA NA 3.94E-07 3.63E-07 3.65E-07 Migration rate from N. pinetum to N. lecontei NA NA 1.64E-08 1.83E-08 1.71E-08 Number of N. pinetum migrants NA NA 0.1273259 0.1226254 0.119698-0.019698-0.0196645 Number of N. lecontei migrants NA NA 0.0181423 0.0196645 0.018665 Time since migration started NA NA 901891 NA NA Time since migration ended NA NA NA 1906 NA Estimated maximum likelihood (log 10) -33034.2 -32805.5 -32794.6 -32795 -32727.9 Maximum observed likelihood (log 10) -32727.9 -32727.9 -32727.9 -32727.9 -32727.9	Admixture proportion from N. lecontei to N. pinetum	NA	0.118292	NA	NA	NA
Migration rate from N. pinetum to N. lecontei NA NA 1.64E-08 1.83E-08 1.71E-08 Number of N. pinetum migrants NA NA 0.1273259 0.1226254 0.1196984 Number of N. lecontei migrants NA NA 0.0181423 0.0196645 0.018665 Time since migration started NA NA 901891 NA NA Time since migration ended NA NA NA 1906 NA Estimated maximum likelihood (log 10) -33034.2 -32805.5 -32794.6 -32795 -32794.3 Maximum observed likelihood (log 10) -32727.9 -32727.9 -32727.9 -32727.9 -32727.9	Time since admixture	NA	115046	NA	NA	NA
Number of N. pinetum migrants NA NA NA 0.1273259 0.1226254 0.1196984 Number of N. lecontei migrants NA NA NA 0.0181423 0.0196645 0.018665 Time since migration started NA NA 901891 NA NA Time since migration ended NA NA NA 1906 NA Estimated maximum likelihood (log 10) -33034.2 -32805.5 -32794.6 -32795 -32794.3 Maximum observed likelihood (log 10) -32727.9 -32727.9 -32727.9 -32727.9 -32727.9	Migration rate from N. lecontei to N. pinetum	NA	NA	3.94E-07	3.63E-07	3.65E-07
Number of N. lecontei migrants NA NA 0.0181423 0.0196645 0.018665 Time since migration started NA NA 901891 NA NA Time since migration ended NA NA NA 1906 NA Estimated maximum likelihood (log 10) -33034.2 -32805.5 -32794.6 -32795 -32794.3 Maximum observed likelihood (log 10) -32727.9 -32727.9 -32727.9 -32727.9 -32727.9	Migration rate from N. pinetum to N. lecontei	NA	NA	1.64E-08	1.83E-08	1.71E-08
Time since migration started NA NA 901891 NA NA Time since migration ended NA NA NA 1906 NA Estimated maximum likelihood (log 10) -33034.2 -32805.5 -32794.6 -32795 -32794.3 Maximum observed likelihood (log 10) -32727.9 -32727.9 -32727.9 -32727.9 -32727.9	Number of N. pinetum migrants	NA	NA	0.1273259	0.1226254	0.1196984
Time since migration ended NA NA NA 1906 NA Estimated maximum likelihood (log 10) -33034.2 -32805.5 -32794.6 -32795 -32794.3 Maximum observed likelihood (log 10) -32727.9 -32727.9 -32727.9 -32727.9 -32727.9	Number of N. lecontei migrants	NA	NA	0.0181423	0.0196645	0.018665
Estimated maximum likelihood (log 10) -33034.2 -32805.5 -32794.6 -32795 -32794.3 Maximum observed likelihood (log 10) -32727.9 -32727.9 -32727.9 -32727.9	Time since migration started	NA	NA	901891	NA	NA
Maximum observed likelihood (log 10) -32727.9 -32727.9 -32727.9 -32727.9 -32727.9	Time since migration ended	NA	NA	NA	1906	NA
	Estimated maximum likelihood (log 10)	-33034.2	-32805.5	-32794.6	-32795	-32794.3
Maximum Likelihood (est-obs) -306.3 -77.6 -66.7 -67.1 -66.4	Maximum observed likelihood (log 10)	-32727.9	-32727.9	-32727.9	-32727.9	-32727.9
· · · · · · · · · · · · · · · · · · ·	Maximum Likelihood (est-obs)	-306.3	-77.6	-66.7	-67.1	-66.4

S3). The increased efficacy of selection and the high probability of allele retention under haplodiploidy and a divergence-withgene-flow scenario is analogous to classical faster-X divergence among isolated populations in which dominance has a large impact on the outcomes (e.g., Charlesworth et al., 1987, 2018; Meisel & Connallon, 2013; Vicoso & Charlesworth, 2009). However, assuming sufficient recombination, differential allele retention during phase 1 has a minimal impact on differentiation at linked neutral sites (e.g., compare Figure 2d,h to Figures 4e and 5e, respectively).

Once populations escape phase 1 without losing the divergently selected allele, there is a second transitional phase during which the increased efficacy of selection against locally maladaptive alleles reduces effective migration rates and causes haplodiploid loci to differentiate more rapidly than comparable diploid loci (Figures 4 and 5). Again, this is in line with classical faster-X theory demonstrating shorter sojourn times for beneficial X-linked alleles in isolated populations (Avery, 1984; Betancourt et al., 2004). Reduced sojourn times in phase 2 also reduce opportunities for recombination between locally adaptive and maladaptive haplotypes, thereby affecting linked variation (Figures 4 and 5), analogous to predictions for X-linked variation in isolated populations (Betancourt et al., 2004; Owen, 1988).

Once diverging populations approach equilibrium between selection, migration and drift, they enter phase 3. In this phase, haplodiploidy increases the efficacy of selection against locally maladapted immigrant alleles, resulting in higher allele frequency differences at hemizygous loci compared to diploid loci (Figures 4 and 5). Consistent with deterministic results obtained under similar demographic models (Lasne et al., 2017), we find that when populations remain connected by gene flow, faster-haplodiploid effects occur irrespective of dominance. These findings contrast with classical faster-X theory that has been developed for divergence in isolation, which predicts increased substitution rate only when beneficial mutations are recessive (e.g., Charlesworth et al., 1987, 2018; Meisel & Connallon, 2013; Vicoso & Charlesworth, 2006) or when codominance is accompanied by deviations from a 50:50 sex ratio (Vicoso & Charlesworth, 2009). Additionally, efficient selection against maladapted migrant alleles in phase 3 causes reduced opportunities for recombination in haplodiploids. This mechanism produces faster-haplodiploid effects at neutral sites linked to both recessive and codominant alleles (Figures 4 and 5). These results are also consistent with predictions from deterministic continent-island models of secondary contact for X-linked markers (Fraïsse & Sachdeva, 2021; Fusco & Uyenoyama, 2011; Muirhead & Presgraves, 2016). Despite several important differences between our model and these secondary contact models, including divergence scenario, migration direction and the presence of drift, we reach qualitatively similar conclusions. These similarities suggest that in the long term, after migration-selection-drift equilibrium is reached, the impact of the initial phases is negligible.

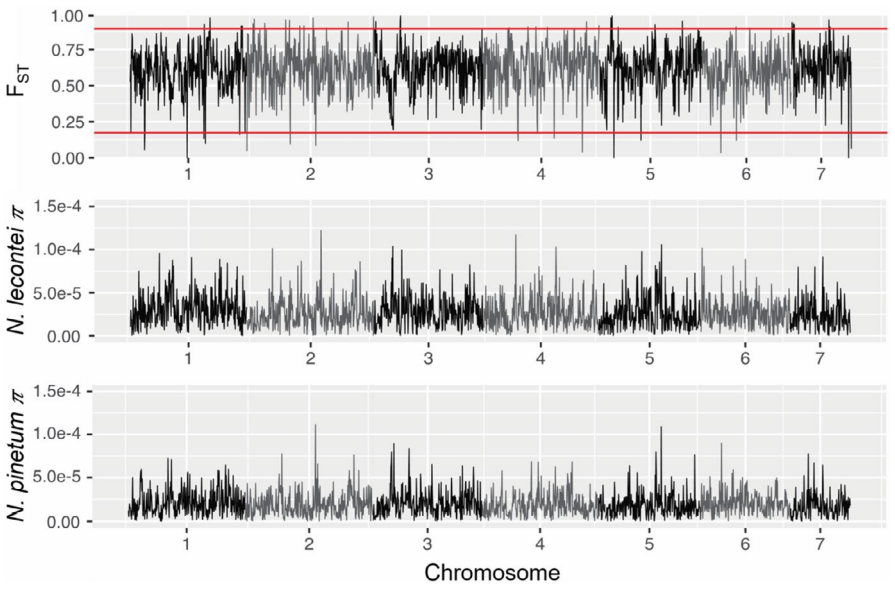


FIGURE 7 Genome scans of differentiation and diversity for Neodiprion pinetum and N. lecontei. Genetic differentiation (F_{ST}) and genetic diversity (nucleotide diversity, π) for N. lecontei and N. pinetum calculated in 100-kb windows. The red lines mark the 95% confidence interval obtained from data simulated under neutrality and the demographic model estimated for this species pair [Colour figure can be viewed at wileyonlinelibrary.com]

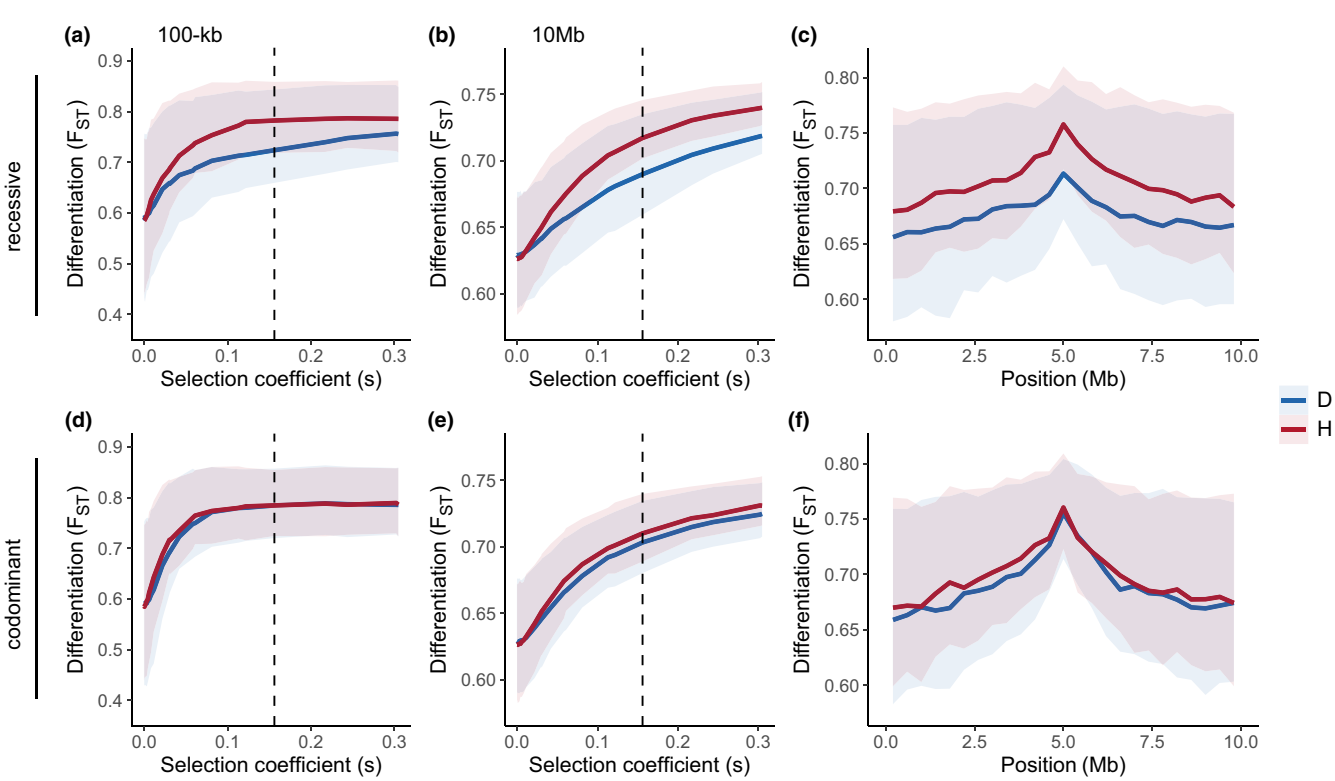


FIGURE 8 Effect of haplodiploidy and divergent selection on differentiation under inferred demographic history of *Neodiprion* sawflies. Results from simulations performed assuming a sex ratio with a proportion of 0.7 females and 0.3 males. (a–b, d–e) Mean F_{ST} and interquartile range for diploid and haplodiploid populations as a function of selective coefficient for recessive (a–b) and codominant (d–e) mutations, for different window sizes centred at the selected site (a,d) 100-kb, (b,e) 10 Mb. (c, f) Genome scan of F_{ST} for diploids and haplodiploids for recessive (c) and codominant (f) mutations, obtained with s=0.16 and initial frequency of 0.1. Solid line corresponds to mean F_{ST} and shaded area indicates interquartile 0.25–0.75 range. Dashed lines in (a–b, d–e) indicate the selective coefficient used in genome scan shown in (c, f). Note that in this model the two populations have different effective sizes (Table S4) and hence the selection coefficients on the x-axis are not scaled by N_e . For s=0.16 this corresponds to scaled selective coefficients of ~2Ns =50 for N. pinetum (where the derived allele is rare initially), and 2Ns=170 for N. lecontei [Colour figure can be viewed at wileyonlinelibrary.com]

Where our work departs most from previous faster-X theory is that—to better connect theory to data—we have explicitly modelled the effects of sex-limited hemizygosity and recombination on population genomic data sets. Here, a couple of surprises have emerged.

First, under some parameter combinations, faster-haplodiploid effects can be observed in loosely linked neutral sites without corresponding effects at the selected site and tightly linked sites (Figure 5h). These patterns, which are dependent on recombination

rate, emerge when haplodiploid populations diverge more rapidly than diploid populations, but ultimately reach the same equilibrium allele frequency. In essence, more rapid differentiation and reduced opportunities for recombination between divergently selected haplotypes in haplodiploids lock linked variation into place, and moderate to strong selection prevents erosion of linkage even with migration. In other words, haplodiploidy leads to larger genomic regions around the selected site with reduced effective migration rate. One important implication of this finding is that haplodiploidy can facilitate the establishment of other beneficial mutations that appear in such genomic regions (Yeaman et al., 2016, see below).

Second, while previous work demonstrates that hemizygous selection will give rise to faster-X effects at selected and linked sites, there has been some uncertainty as to how much of the genome is likely to be impacted when there is recurrent migration (Presgraves, 2018). Here, we show that with strong selection (2Ns > 100) and high migration (2Nm ~5), regions of elevated differentiation in haplodiploid chromosomes will be higher and wider than in corresponding diploid chromosomes. Moreover, divergent selection at a single haplodiploid locus can reduce gene flow relative to the diploid case even at neutral sites more than 250 kb away, corresponding to >4.40 cM in simulations under the symmetric isolation-with-migration model (Figures 4 and 5), or >21.5 cM in simulations with sawfly-specific parameters (Figure 8). Additionally, the continent-island models of Fusco and Uyenoyama (2011) and Muirhead and Presgraves (2016) predict that selection at X-linked (and, analogously, haplodiploid) sites can also impact unlinked neutral markers. Assuming that, at equilibrium, adaptive divergence-with-gene-flow dynamics can be reasonably well approximated by the continent-island model, we speculate that localized reductions in gene flow surrounding hemizygous loci could extend to the chromosome-wide level.

Although our work better connects theory to empirical data, our models make several simplifying assumptions that could impact patterns of faster-haplodiploid differentiation. Relaxing these assumptions and creating more complex, but realistic, models are therefore potentially fruitful avenues for future research. First, the genetic architecture of adaptation to novel niches is probably much more complex than the simple single-locus model considered here (i.e., adaptation is likely to be due to many loci with variable effect sizes, dominance coefficients and nonadditive interactions). Although there has been some work on how divergent selection on multiple, possibly interacting, loci impact genomic differentiation (e.g., Aeschbacher et al., 2017; Yeaman et al., 2016), this has not been investigated in the context of hemizygosity (but see Fraïsse & Sachdeva, 2021; Fusco & Uyenoyama, 2011). Second, the divergence model we considered was also relatively simple, ignoring sex-specific effects such as sex-biased migration, sex-specific selection and the absence of dosage compensation. For instance, Lasne et al. (2017) predicted that sex-specific migration has a large impact on faster-X effects in models with strong migration (m» s). Third, we have considered a parallel dominance fitness landscape, and the magnitude of faster-X effects might differ for other models, although Lasne et al. (2017) found similar

results for both parallel and reversal dominance models. Fourth, we assumed that the fitness of haploid males was equivalent to that of diploid homozygotes. Whether this is the case depends on mechanisms of dosage compensation and allelic effects in haploid males, which are not well understood (Gardner, 2012; Hitchcock et al., 2022; but see Aron et al., 2005; Dearden et al., 2006; Glastad et al., 2014). Finally, we have ignored the effects that removing deleterious mutations with similar effects across populations may have on patterns of differentiation in haplodiploids and diploids (Charlesworth et al., 1993, 1997). Making precise predictions about chromosome-wide levels in population genomic data sets will require modelling these more complex scenarios, as well as considering local variation in mutation and recombination rate.

4.2 | Implications for speciation in haplodiploids

One of the longest running debates in evolutionary biology is over the plausibility and prevalence of sympatric speciation, the evolution of reproductive isolation in the absence of geographical isolation (Berlocher & Feder, 2002; Bolnick & Fitzpatrick, 2007; Foote, 2018; Via, 2001). Because of their pronounced host specialization and lifelong association with their host plants, Neodiprion sawflies have been hypothesized to undergo sympatric speciation (Bush, 1975a, 1975b; Knerer & Atwood, 1973; Linnen & Farrell, 2010). Although gene flow has been ubiquitous throughout Neodiprion divergence (Linnen & Farrell, 2007) and N. pinetum's range is nested within that of N. lecontei, species ranges have changed too much to reconstruct the geographical context of speciation from present-day range overlap (Linnen & Farrell, 2010). Here, demographic modelling revealed that the model that best explains patterns of genomic variation in N. lecontei and N. pinetum does not include a period of isolation (Table 1; Figure 6c). However, distinguishing between models of sympatric divergence and secondary contact is difficult (Sousa & Hey, 2013). This difficulty appears to be true for N. lecontei and N. pinetum as well: models that included continuous migration either starting after a brief period of isolation (~64,000 generations) or ending just before the present day (~2,000 generations) explained the data nearly as well as a continuous migration model (Table 1). Although we cannot definitively say speciation was sympatric, our top three models and maximumlikelihood parameter estimates all point to a scenario in which gene flow was present throughout all or most of the divergence history of these two species.

Previous work also demonstrates that differences in the pines that *N. lecontei* and *N. pinetum* use are likely to generate divergent selection on many different types of traits, including female oviposition traits, correlated male traits and larval physiology (Bendall et al., 2017, 2020; Benjamin, 1955; Coppel & Benjamin, 1965; Rauf & Benjamin, 1980; Wilson et al., 1992). Consistent with a "multifarous" or "multidimensional" model of divergent selection (Feder & Nosil, 2010; Rice & Hostert, 1993; White & Butlin, 2021), multiple unlinked loci exceeded expected levels of differentiation

on non-neutral linked variation and interactions between multiple loci (Feder, Gejji, et al., 2012; Feder & Nosil, 2010; Flaxman et al., 2012; Nosil & Feder, 2012; Via, 2012; Yeaman et al., 2016; Yeaman & Whitlock, 2011).

under neutrality (Figure 7). We also observed multiple regions of unusually low differentiation, which could be explained by adaptive introgression. We acknowledge, however, that other mechanisms besides divergent selection and adaptive introgression can cause dips and valleys in genome scans (Cruickshank & Hahn, 2014; Ravinet et al., 2017). Thus, interpretation of these genome scans would be improved by characterizing the genomic landscape of recombination and gene density, as well as mapping loci underlying divergently selected traits.

Together with previous work characterizing reproductive barriers in this species pair (Bendall et al., 2017), our demographic modelling and genome scan results support a scenario in which adaptation to different pine trees drove the evolution of reproductive isolation in the presence of substantial gene flow. There is little debate that, given sufficiently strong selection, genetic and phenotypic differences, such as divergently selected hostuse traits, can be maintained in the face of gene flow. Instead, the primary objection to sympatric speciation has been that gene flow and recombination will tend to break up associations among favourable combinations of alleles and between divergently selected loci and loci that confer other components of reproductive isolation (Felsenstein, 1981). Multiple mechanisms can help overcome this "selection-recombination" antagonism, thereby aiding the evolution of reproductive isolation when there is gene flow, including pleiotropy ("magic traits" wherein loci underlying local adaptation also confer reproductive isolation; Servedio et al., 2011) and genomic features that reduce recombination (e.g., chromosome inversions; Kirkpatrick & Barton, 2006; Ravinet et al., 2017). Because Neodiprion mate on the host plant, it is possible that alleles underlying divergent host preferences also produce habitat isolation (Linnen & Farrell, 2010). However, there is minimal evidence of chromosomal rearrangements that would reduce recombination in N. lecontei-N. pinetum hybrids (S. Geib and S. Sim, personal communication).

Even in the absence of "magic traits" and inversions, divergent selection can also facilitate the evolution of reproductive isolation through effects on linked variation (divergence hitchhiking; Via, 2009; Via & West, 2008) and, when there are multiple divergently selected loci, via a genome-wide reduction in the effective migration rate (genome hitchhiking; Barton & Bengtsson, 1986; Feder et al., 2012a, 2012b; Flaxman et al., 2012, 2013). By simulating genomic differentiation under divergent selection, our estimated demographic model and other system-specific details (sex ratio, recombination rate), we show that haplodiploid inheritance in N. lecontei and N. pinetum probably increased differentiation at selected and linked loci relative to a comparable diploid scenario (Figure 8). The impact of haplodiploidy was most pronounced for recessive mutations and at intermediate selection coefficients, with effects extending over sizable regions of the genome (comparable to ~10 Mb). By increasing differentiation at linked sites, haplodiploidy could facilitate both divergence hitchhiking and genome hitchhiking, thereby promoting speciation-with-gene-flow. This hypothesis could be tested more directly via simulations that examine the impact of haplodiploidy

4.3 | Conclusions

Overall, our work suggests that sex-limited hemizygosity and recombination, both of which are maximized in Hymenoptera and other haplodiploid clades, can have substantial effects on genomic differentiation in wild populations. One potential implication of this work is that haplodiploid taxa are more likely to undergo sympatric speciation and can withstand greater levels of gene flow during divergence, which may ultimately give rise to higher rates of local adaptation and speciation. A comparative analysis of divergence history between diploids and haplodiploids would be an informative step in testing this hypothesis. More generally, there are potentially numerous evolutionary consequences of haplodiploidy that may shed light on patterns of biodiversity and have implications that extend to nonhaplodiploid taxa.

ACKNOWLEDGEMENTS

We thank members of the Linnen laboratory for assistance with collection and rearing of pine sawflies, and we thank Kim Vertacnik for providing data from an outgroup taxon. We also thank three anonymous reviewers for constructive feedback. This work was supported by the National Science Foundation (DEB-CAREER-1750946 and DEB-1257739 to C.R.L); USDA-NIFA predoctoral fellowship (2015-67011-22803 to R.K.B.); Portuguese National Science Foundation ("Fundação para a Ciência e a Tecnologia"-FCT; UIDB/00329/2020, individual grants CEECIND/02391/2017 and CEECINST/00032/2018/CP1523/CT0008 to V.C.S.); and by the EU H2020 programme (Marie Skłodowska-Curie grant no. 799729 to V.C.S.). For computing resources, we thank the University of Kentucky Center for Computational Sciences and the Lipscomb High Performance Computing Cluster, as well as the INCD (https://incd. pt/), access to which was funded through FCT Advanced Computing Projects (CPCA/A0/7303/2020 to V.C.S.).

AUTHOR CONTRIBUTIONS

E.E.B., V.C.S. and C.R.L. designed the research; E.E.B., V.C.S., R.K.B. and C.R.L. performed the research; E.E.B., V.C.S. and C.R.L. analysed the data; E.E.B., V.C.S. and C.R.L. wrote the paper, with input from all authors.

OPEN RESEARCH BADGES



This article has earned an Open Data Badge for making publicly available the digitally-shareable data necessary to reproduce the reported results. The data is available at VCS's GitHub page (https://github.com/vsousa/EG_cE3c).

DATA AVAILABILITY STATEMENT

All the scripts used for SLIM version 3 simulations (bash and Slim input files) and analysis of SLIM results (R scripts) are available on VCS's GitHub page (https://github.com/vsousa/EG_cE3c). *Neodiprion* sequencing reads are available via the NCBI SRA, accession nos.: SAMN23893940–SAMN23893944, SAMN23893965, and SAMN23893960–SAMN23893963, SAMN23893965, and SAMN25157024–SAMN25157101. All VCF files, custom scripts and input files for the analysis of sawfly data are available on DRYAD (https://doi.org/10.5061/dryad.fbg79cnwx).

ORCID

Emily E. Bendall https://orcid.org/0000-0003-2524-088X

Robin K. Bagley https://orcid.org/0000-0003-2209-0521

Vitor C. Sousa https://orcid.org/0000-0003-3575-0875

Catherine R. Linnen https://orcid.org/0000-0001-5715-456X

REFERENCES

- Aeschbacher, S., Selby, J. P., Willis, J. H., & Coop, G. (2017). Populationgenomic inference of the strength and timing of selection against gene flow. *Proceedings of the National Academy of Sciences*, 114(27), 7061–7066. https://doi.org/10.1073/pnas.1616755114
- Alexander, D. H., Novembre, J., & Lange, K. (2009). Fast model-based estimation of ancestry in unrelated individuals. *Genome Research*, 19, 1655–1664. https://doi.org/10.1101/gr.094052.109
- Aron, S., de Menten, L., van Bockstaele, D. R., Blank, S. M., & Roisin, Y. (2005). When hymenopteran males reinvented diploidy. *Current Biology*, 15(9), 824–827. https://doi.org/10.1016/J.CUB.2005.03.017
- Avery, P. J. (1984). The population genetics of haplo-diploids and X-linked genes. *Genetical Research*, 44(3), 321–341. https://doi.org/10.1017/S0016672300026550
- Bagley, R. K., Sousa, V. C., Niemiller, M. L., & Linnen, C. R. (2017). History, geography and host use shape genomewide patterns of genetic variation in the redheaded pine sawfly (*Neodiprion lecontei*). *Molecular Ecology*, 26(4), 1022–1044. https://doi.org/10.1111/mec.13972
- Barton, N. H., & Bengtsson, B. O. (1986). The barrier to genetic exchange between hybridising populations. *Heredity*, 56(3), 357–376. https://doi.org/10.1038/hdy.1986.135
- Bendall, E. E., Mattingly, K. M., Moehring, A. J., & Linnen, C. R. (2020). Lack of intrinsic postzygotic isolation in haplodiploid male hybrids despite high genetic distance. *BioRxiv*, 2020.01.08.898957. https://doi.org/10.1101/2020.01.08.898957
- Bendall, E. E., Vertacnik, K. L., & Linnen, C. R. (2017). Oviposition traits generate extrinsic postzygotic isolation between two pine sawfly species. *BMC Evolutionary Biology*, 17(1), 1–15. https://doi.org/10.1186/s12862-017-0872-8
- Benjamin, D. M. (1955). The Biology and Ecology of the Red-headed Pine Sawfly. U.S. Department of Agriculture.
- Berlocher, S., & Feder, J. (2002). Sympatric speciation in phytophagous insects: moving beyond controversy? *Annual Review of Entomology*, 47, 773–815. https://doi.org/10.1146/ANNUR EV.ENTO.47.091201.145312
- Betancourt, A. J., Kim, Y., & Orr, H. A. (2004). A pseudohitchhiking model of X vs. autosomal diversity. *Genetics*, 168(4), 2261–2269. https://doi.org/10.1534/genetics.104.030999
- Bhatia, G., Patterson, N., Sankararaman, S., & Price, A. L. (2013). Estimating and interpreting FST: the impact of rare variants. *Genome Research*, 23(9), 1514–1521. https://doi.org/10.1101/gr.154831.113

- Blackmon, H., Ross, L., & Bachtrog, D. (2017). Sex determination, sex chromosomes, and karyotype evolution in insects. *Journal of Heredity*, 108(1), 78–93. https://doi.org/10.1093/jhered/esw047
- Bolnick, D. I., & Fitzpatrick, B. M. (2007). Sympatric speciation: Models and empirical evidence. Annual Review of Ecology, Evolution, and Systematics, 38, 459-487. https://doi.org/10.1146/annurev.ecols vs.38.091206.095804
- Boulton, R. A., Collins, L. A., & Shuker, D. M. (2015). Beyond sex allocation: the role of mating systems in sexual selection in parasitoid wasps. *Biological Reviews*, 90(2), 599–627. https://doi.org/10.1111/BRV.12126
- Burford Reiskind, M. O., Coyle, K., Daniels, H. V., Labadie, P., Reiskind, M. H., Roberts, N. B., Schaff, J., & Vargo, E. L. (2016). Development of a universal double-digest RAD sequencing approach for a group of nonmodel, ecologically and economically important insect and fish taxa. *Molecular Ecology Resources*, 16(6), 1303–1314. https://doi.org/10.1111/1755-0998.12527
- Bush, G. L. (1975). Modes of animal speciation. *Annual Review of Ecology and Systematics*, 6(1), 339–364. https://doi.org/10.1146/annurev.es.06.110175.002011
- Bush, G. L. (1975). Sympatric speciation in phytophagous parasitic insects. In P. W. Price (Ed.), Evolutionary Strategies of Parasitic Insects and Mites (pp. 187–206). Springer. https://doi.org/10.1007/978-1-4615-8732-3_9
- Charlesworth, B. (2012). The role of background selection in shaping patterns of molecular evolution and variation: evidence from variability on the *Drosophila X* Chromosome. *Genetics*, 191(1), 233–246. https://doi.org/10.1534/genetics.111.138073
- Charlesworth, B., Campos, J. L., & Jackson, B. C. (2018). Faster-X evolution: Theory and evidence from *Drosophila*. *Molecular Ecology*, 27(19), 3753–3771. https://doi.org/10.1111/mec.14534
- Charlesworth, B., Coyne, J. A., & Barton, N. H. (1987). The relative rates of evolution of sex chromosomes and autosomes. *The American Naturalist*, 130(1), 113–146. https://doi.org/10.1086/284701
- Charlesworth, B., Morgan, M. T., & Charlesworth, D. (1993). The effect of deleterious mutations on neutral molecular variation. *Genetics*, 134(4), 1289–1303. https://doi.org/10.1093/genetics/134.4.1289
- Charlesworth, B., Nordborg, M., & Charlesworth, D. (1997). The effects of local selection, balanced polymorphism and background selection on equilibrium patterns of genetic diversity in subdivided populations. *Genetical Research*, 70(2), 155–174.
- Chen, H., Rangasamy, M., Tan, S. Y., Wang, H., & Siegfried, B. D. (2010). Evaluation of five methods for total DNA extraction from western corn rootworm beetles. *PLoS One*, 5(8), e11963. https://doi.org/10.1371/journal.pone.0011963
- Codella, S. G., & Raffa, K. F. (2002). Desiccation of *Pinus* foliage induced by conifer sawfly oviposition: effect on egg viability. *Ecological Entomology*, 27(5), 618–621. https://doi.org/10.1046/j.1365-2311.2002.00447.x
- Coppel, H., & Benjamin, D. (1965). Bionomics of the Nearctic pine-feeding diprionids. *Annual Review of Entomology*, 10, 69–96. https://doi.org/10.1146/annurev.en.10.010165.000441
- Craig, T. P., & Mopper, S. (1993). Sex ratio variation in sawflies. In M. Wagner, & K. F. Raffa (Eds.), Sawfly Life History Adaptations to Woody Plants (pp. 61-92). Academic Press.
- Cruickshank, T. E., & Hahn, M. W. (2014). Reanalysis suggests that genomic islands of speciation are due to reduced diversity, not reduced gene flow. *Molecular Ecology*, 23(13), 3133–3157. https://doi.org/10.1111/mec.12796
- Curtsinger, J. W., Service, P. M., & Prout, T. (1994). Antagonistic pleiotropy, reversal of dominance, and genetic polymorphism. *The American Naturalist*, 144(2), 210–228. https://doi.org/10.1086/285671
- Danecek, P., Auton, A., Abecasis, G., Albers, C. A., Banks, E., DePristo, M. A., Handsaker, R. E., Lunter, G., Marth, G. T., Sherry, S. T., McVean, G., & Durbin, R. (2011). The variant call format and VCFtools.

- Bioinformatics, 27(15), 2156-2158. https://doi.org/10.1093/bioin formatics/btr330
- Davies, N. G., & Gardner, A. (2014). Evolution of paternal care in diploid and haplodiploid populations. Journal of Evolutionary Biology, 27(6), 1012-1019. https://doi.org/10.1111/jeb.12375
- de la Filia, A. G., Bain, S. A., & Ross, L. (2015). Haplodiploidy and the reproductive ecology of Arthropods. Current Opinion in Insect Science, 9, 36-43. https://doi.org/10.1016/j.cois.2015.04.018
- Dearden, P. K., Wilson, M. J., Sablan, L., Osborne, P. W., Havler, M., McNaughton, E., Kimura, K., Milshina, N. V., Hasselmann, M., Gempe, T., Schioett, M., Brown, S. J., Elsik, C. G., Holland, P. W. H., Kadowaki, T., & Beye, M. (2006). Patterns of conservation and change in honey bee developmental genes. Genome Research, 16(11), 1376-1384. https://doi.org/10.1101/gr.5108606
- Excoffier, L., Dupanloup, I., Huerta-Sánchez, E., Sousa, V. C., & Foll, M. (2013). Robust demographic inference from genomic and SNP data. PLoS Genetics, 9(10), e1003905. https://doi.org/10.1371/journ al.pgen.1003905
- Feder, J. L., Egan, S. P., & Nosil, P. (2012). The genomics of speciationwith-gene-flow. Trends in Genetics, 28(7), 342-350. https://doi. org/10.1016/j.tig.2012.03.009
- Feder, J. L., Gejji, R., Yeaman, S., & Nosil, P. (2012). Establishment of new mutations under divergence and genome hitchhiking. Philosophical Transactions of the Royal Society B: Biological Sciences, 367(1587), 461-474. https://doi.org/10.1098/rstb.2011.0256
- Feder, J. L., & Nosil, P. (2010). The efficacy of divergence hitchhiking in generating genomic islands during ecological speciation. Evolution, 64(6), 1729-1747. https://doi.org/10.1111/j.1558-5646.2009.00943.x
- Felsenstein, J. (1981). Skepticism towards Santa Rosalia, or why are there so few kinds of animals? Evolution, 35(1), 124-138. https://doi. org/10.1111/j.1558-5646.1981.tb04864.x
- Flaxman, S. M., Feder, J. L., & Nosil, P. (2012). Spatially explicit models of divergence and genome hitchhiking. Journal of Evolutionary Biology, 25(12), 2633-2650. https://doi.org/10.1111/JEB.12013
- Flaxman, S. M., Feder, J. L., & Nosil, P. (2013). Genetic hitchhiking and the dynamic buildup of genomic divergence during speciation with gene flow. Evolution, 67(9), 2577-2591. https://doi.org/10.1111/ evo.12055
- Foote, A. D. (2018). Sympatric Speciation in the Genomic Era. Trends in Ecology and Evolution, 33(2), 85-95. https://doi.org/10.1016/j. tree.2017.11.003
- Forbes, A. A., Bagley, R. K., Beer, M. A., Hippee, A. C., & Widmayer, H. A. (2018). Quantifying the unquantifiable: why Hymenoptera, not Coleoptera, is the most speciose animal order. BMC Ecology, 18(1), 1-11. https://doi.org/10.1186/s12898-018-0176-x
- Fraïsse, C., & Sachdeva, H. (2021). The rates of introgression and barriers to genetic exchange between hybridizing species: sex chromosomes vs autosomes. Genetics, 217(2), iyaa025.
- Frank, S. A. (1991). Divergence of meiotic drive-suppression systems as an explanation for sex-biased hybrid sterility and inviability. Evolution, 45(2), 262-267. https://doi.org/10.1111/j.1558-5646.1991.tb044 01.x
- Fusco, D., & Uyenoyama, M. K. (2011). Sex-specific incompatibility generates locus-specific rates of introgression between species. Genetics, 189(1), 267-288. https://doi.org/10.1534/genetics.111.130732
- Gardner, A. (2012). Evolution of maternal care in diploid and haplodiploid populations. Journal of Evolutionary Biology, 25(8), 1479-1486. https://doi.org/10.1111/j.1420-9101.2012.02551.x
- Ghenu, A.-H., Blanckaert, A., Butlin, R. K., Kulmuni, J., & Bank, C. (2018). Conflict between heterozygote advantage and hybrid incompatibility in haplodiploids (and sex chromosomes). Molecular Ecology, 27(19), 3935-3949. https://doi.org/10.1111/mec.14482
- Glastad, K. M., Hunt, B. G., Yi, S. V., & Goodisman, M. A. D. (2014). Epigenetic inheritance and genome regulation: is DNA methylation linked to ploidy in haplodiploid insects? Proceedings of the Royal

- Society B: Biological Sciences, 281(1785), 20140411. https://doi. org/10.1098/RSPB.2014.0411
- Haller, B. C., & Messer, P. W. (2019). SLiM 3: forward genetic simulations beyond the wright-fisher model. Molecular Biology and Evolution, 36(3), 632-637. https://doi.org/10.1093/molbev/msy228
- Hamilton, W. D. (1964a). The genetical evolution of social behaviour. I. Journal of Theoretical Biology, 7(1), 1-16. https://doi. org/10.1016/0022-5193(64)90038-4
- Hamilton, W. D. (1964b). The genetical evolution of social behaviour. II. Journal of Theoretical Biology, 7(1), 17-52. https://doi. org/10.1016/0022-5193(64)90039-6
- Hamilton, W. D. (1967). Extraordinary sex ratios. Science, 156(3774), 477-488. https://doi.org/10.1126/science.156.3774.477
- Hamilton, W. D. (1972). Altruism and Related Phenomena. Annual Review of Ecological Systems, 3, 193-232.
- Harper, K. E., Bagley, R. K., Thompson, K. L., & Linnen, C. R. (2016). Complementary sex determination, inbreeding depression and inbreeding avoidance in a gregarious sawfly. Heredity, 117(5), 326-335. https://doi.org/10.1038/hdy.2016.46
- Hartl, D. L. (1972). A Fundamental Theorem of Natural Selection for Sex Linkage or Arrhenotoky. The American Naturalist, 106(950), 516-524. https://doi.org/10.1086/282791
- Hedrick, P. W., & Parker, J. D. (1997). Evolutionary Genetics and Genetic Variation of Haplodiploids and X-Linked Genes. Annual Review of Ecology and Systematics, 28, 55-83. https://doi.org/10.1146/annur ev.ecolsys.28.1.55
- Hey, J., & Pinho, C. (2012). Population genetics and objectivity in species diagnosis. Evolution, 66(5), 1413-1429. https://doi. org/10.1111/j.1558-5646.2011.01542.x
- Hitchcock, T., Gardner, A., & Ross, L. (2022). Sexual antagonism in haplodiploids. Evolution, 76(2), 292-308. https://doi.org/10.1111/ evo.14398
- Hoban, S., Bertorelle, G., & Gaggiotti, O. E. (2012). Computer simulations: tools for population and evolutionary genetics. Nature Reviews Genetics, 13(2), 110-122. https://doi.org/10.1038/nrg3130
- Hölldobler, B., & Wilson, E. O. (1990). The Ants. Cambridge. Harvard University Press. Retrieved from. https://doi.org/10.1007/978-3-662-10306-7
- Hurst, L. D., & Pomiankowski, A. (1991). Causes of sex ratio bias may account for unisexual sterility in hybrids: a new explanation of Haldane's rule and related phenomena. Genetics, 128(4), 841-858. https://doi.org/10.1093/genetics/128.4.841
- Irwin, D. E. (2018). Sex chromosomes and speciation in birds and other ZW systems. Molecular Ecology, 27(19), 3831-3851. https://doi. org/10.1111/mec.14537
- Kirkpatrick, M., & Barton, N. (2006). Chromosome inversions, local adaptation and speciation. Genetics, 173(1), 419-434. https://doi. org/10.1534/genetics.105.047985
- Kirkpatrick, M., & Hall, D. W. (2004). Sexual selection and sex linkage. Evolution, 683-691. 58(4). https://doi.org/10.1111/ j.0014-3820.2004.tb00401.x
- Klein, K., Kokko, H., & ten Brink, H.. (2021). Disentangling verbal arguments: Intralocus sexual conflict in haplodiploids. American Naturalist, 198(6), 678-693. https://doi.org/10.1086/716908/ ASSET/IMAGES/LARGE/FG4.JPEG
- Knerer, G., & Atwood, C. E. (1973). Diprionid sawflies: Polymorphism and speciation. Science, 179(4078), 1090-1099. https://doi. org/10.1126/science.179.4078.1090
- Koevoets, T., & Beukeboom, L. W. (2008). Genetics of postzygotic isolation and Haldane's rule in haplodiploids. Heredity, 102(1), 16-23. https://doi.org/10.1038/hdy.2008.44
- Kong, A., Gudbjartsson, D. F., Sainz, J., Jonsdottir, G. M., Gudjonsson, S. A., Richardsson, B., & Stefansson, K. (2002). A high-resolution recombination map of the human genome. Nature Genetics, 31(3), 241-247. https://doi.org/10.1038/ng917

- Kraaijeveld, K. (2009). Male genes with nowhere to hide sexual conflict in haplodiploids. Animal Biology, 59(4), 403-415. https://doi. org/10.1163/157075509X12499949744225
- Langmead, B., & Salzberg, S. L. (2012). Fast gapped-read alignment with Bowtie 2. Nature Methods, 9(4), 357-359. https://doi.org/10.1038/ nmeth.1923
- Lasne, C., Sgrò, C. M., & Connallon, T. (2017). The Relative Contributions of the X Chromosome and Autosomes to Local Adaptation. Genetics. 205(3), 1285-1304. https://doi.org/10.1534/genetics.116.194670
- Lester, L. J., & Selander, R. K. (1979). Population genetics of haplodiploid insects. Genetics, 92(4), 1329-1345. https://doi.org/10.1093/genet ics/92.4.1329
- Li, H., Handsaker, B., Wysoker, A., Fennell, T., Ruan, J., Homer, N., & Durbin, R. (2009). The Sequence Alignment/Map format and SAMtools. Bioinformatics, 25(16), 2078-2079. https://doi. org/10.1093/bioinformatics/btp352
- Lindstedt, C., Bagley, R., Calhim, S., Jones, M., & Linnen, C. R. (2022). The impact of life stage and pigment source on the evolution of novel warning signal traits. Evolution, in Press, https://doi.org/10.1111/ evo.14443
- Linnen, C. R., & Farrell, B. D. (2007). Mitonuclear discordance is caused by rampant mitochondrial introgression in Neodiprion (Hymenoptera: Diprionidae) sawflies. Evolution, 61(6), 1417-1438. https://doi. org/10.1111/j.1558-5646.2007.00114.x
- Linnen, C. R., & Farrell, B. D. (2008). Comparison of methods for speciestree inference in the sawfly genus Neodiprion (Hymenoptera: Diprionidae). Systematic Biology, 57(6), 876-890. https://doi. org/10.1080/10635150802580949
- Linnen, C. R., & Farrell, B. D. (2010). A test of the sympatric host race formation hypothesis in Neodiprion (Hymenoptera: Diprionidae). Proceedings of the Royal Society B: Biological Sciences, 277(1697), 3131-3138. https://doi.org/10.1098/rspb.2010.0577
- Linnen, C. R., O'Quin, C. T., Shackleford, T., Sears, C. R., & Lindstedt, C. (2018). Genetic basis of body color and spotting pattern in redheaded pine sawfly larvae (Neodiprion lecontei). Genetics, 209(1), 291-305. https://doi.org/10.1534/genetics.118.300793
- Lohse, K., & Ross, L. (2015). What haplodiploids can teach us about hybridization and speciation. Molecular Ecology, 24(20), 5075-5077. https://doi.org/10.1111/mec.13393
- Martin, M. (2011). Cutadapt removes adapter sequences from highthroughput sequencing reads | Martin | EMBnet.journal. EMBnet. Journal, 1, 10-12. https://doi.org/10.14806/ej.17.1.200
- Meiklejohn, C. D., Landeen, E. L., Gordon, K. E., Rzatkiewicz, T., Kingan, S. B., Geneva, A. J., Vedanayagam, J. P., Muirhead, C. A., Garrigan, D., Stern, D. L., & Presgraves, D. C. (2018). Gene flow mediates the role of sex chromosome meiotic drive during complex speciation. eLife, 7, e35468. https://doi.org/10.7554/eLife.35468
- Meisel, R. P., & Connallon, T. (2013, September). The faster-X effect: Integrating theory and data. Trends in Genetics, 29, 537-544. https://doi.org/10.1016/j.tig.2013.05.009
- Moran, P. (1959). The Theory of Some Genetical Effects of Population Subdivision. Australian Journal of Biological Sciences, 12(2), 109. https://doi.org/10.1071/bi9590109
- Muirhead, C. A., & Presgraves, D. C. (2016). Hybrid Incompatibilities, Local Adaptation, and the Genomic Distribution of Natural Introgression between Species. The American Naturalist, 187(2), 249-261. https://doi.org/10.1086/684583
- Normark, B. B. (2003). November 28). The Evolution of Alternative Genetic Systems in Insects. Annual Review of Entomology, 48, 397-423. https://doi.org/10.1146/annurev.ento.48.091801.112703
- Nosil, P., & Feder, J. L. (2012). Genomic divergence during speciation: Causes and consequences. Philosophical Transactions of the Royal Society B: Biological Sciences, 367(1587), 332-342. https://doi. org/10.1098/rstb.2011.0263
- Nouhaud, P., Blanckaert, A., Bank, C., & Kulmuni, J. (2020, January 1). Understanding admixture: Haplodiploidy to the rescue. Trends

- in Ecology and Evolution, 35, 34-42. https://doi.org/10.1016/j. tree.2019.08.013
- Owen, R. E. (1986). Gene frequency dines at X-linked or haplodiploid loci. Heredity, 57(2), 209-219. https://doi.org/10.1038/hdy.1986.111
- Owen, R. E. (1988). Selection at two sex-linked loci. Heredity, 60(3), 415-425. https://doi.org/10.1038/hdv.1988.59
- Patten, M. M. (2018). Selfish X chromosomes and speciation. Molecular Ecology, 27(19), 3772-3782. https://doi.org/10.1111/mec.14471
- Patten, M. M., Carioscia, S. A., & Linnen, C. R. (2015). Biased introgression of mitochondrial and nuclear genes: A comparison of diploid and haplodiploid systems. Molecular Ecology, 24(20), 5200-5210. https://doi.org/10.1111/mec.13318
- Patterson, N. J., Moorjani, P., Luo, Y., Mallick, S., Rohland, N., Zhan, Y., Genschoreck, T., Webster, T., & Reich, D. (2012). Ancient admixture in human history. Genetics, 192(3), 1065-1093. https://doi. org/10.1534/genetics.112.145037
- Peterson, B. K., Weber, J. N., Kay, E. H., Fisher, H. S., & Hoekstra, H. E. (2012). Double digest RADseq: An inexpensive method for de novo SNP discovery and genotyping in model and non-model species. PLoS One, 7(5), e37135. https://doi.org/10.1371/journ al.pone.0037135
- Phung, T. N., Huber, C. D., & Lohmueller, K. E. (2016). Determining the Effect of Natural Selection on Linked Neutral Divergence across Species. PLOS Genetics, 12(8), e1006199. https://doi.org/10.1371/ JOURNAL.PGEN.1006199
- Pinho, C., & Hey, J. (2010). Divergence with Gene Flow: Models and Data. Annual Review of Ecology, Evolution, and Systematics, 41(1), 215–230. https://doi.org/10.1146/annurev-ecolsys-102209-144644
- Presgraves, D. C. (2018). Evaluating genomic signatures of "the large Xeffect" during complex speciation. Molecular Ecology, 27(19), 3822-3830. https://doi.org/10.1111/mec.14777
- Rauf, A., & Benjamin, D. M. (1980). The biology of the white pine sawfly, Neodiprion pinetum (Hymenoptera: Diprionidae) in Wisconsin. The Great Lakes Entomologist, 13(4), 219-224.
- Rautiala, P., Helanterä, H., & Puurtinen, M. (2019). Extended haplodiploidy hypothesis. Evolution Letters, 3(3), 263-270. https://doi. org/10.1002/evl3.119
- Ravinet, M., Faria, R., Butlin, R. K., Galindo, J., Bierne, N., Rafajlović, M., & Westram, A. M. (2017). Interpreting the genomic landscape of speciation: a road map for finding barriers to gene flow. Journal of Evolutionary Biology, 30(8), 1450-1477. https://doi.org/10.1111/jeb.13047
- Reeve, H. K., & Pfennig, D. W. (2003). Genetic biases for showy males: Are some genetic systems especially conducive to sexual selection? Proceedings of the National Academy of Sciences, 100(3), 1089-1094. https://doi.org/10.1073/PNAS.0337427100
- Rice, W., & Hostert, E. (1993). Laboratory experiments on speciation: what have we learned in 40 years? Evolution; International Journal of Organic Evolution, 47(6), 1637-1653. https://doi.org/10.1111/ J.1558-5646.1993.TB01257.X
- Rosenblum, E. B., Römpler, H., Schöneberg, T., & Hoekstra, H. E. (2010). Molecular and functional basis of phenotypic convergence in white lizards at White Sands. Proceedings of the National Academy of Sciences of the United States of America, 107(5), 2113-2117. https:// doi.org/10.1073/pnas.0911042107
- Schweyen, H., Rozenberg, A., & Leese, F. (2014). Detection and Removal of PCR Duplicates in Population Genomic ddRAD Studies by Addition of a Degenerate Base Region (DBR) in Sequencing Adapters. The Biological Bulletin, 227(2), 146-160. https://doi. org/10.1086/BBLv227n2p146
- Servedio, M. R., van Doorn, G. S., Kopp, M., Frame, A. M., & Nosil, P. (2011). Magic traits in speciation: 'magic' but not rare? Trends in Ecology & Evolution, 26(8), 389-397. https://doi.org/10.1016/J. TREE.2011.04.005
- Sousa, V., & Hey, J. (2013). Understanding the origin of species with genome-scale data: Modelling gene flow. Nature Reviews Genetics, 14(6), 404-414. https://doi.org/10.1038/nrg3446

- Staab, P. R., Zhu, S., Metzler, D., & Lunter, G. (2015). scrm: efficiently simulating long sequences using the approximated coalescent with recombination. *Bioinformatics*, 31(10), 1680–1682. https://doi.org/10.1093/BIOINFORMATICS/BTU861
- Terasaki Hart, D. E., Bishop, A. P., & Wang, I. J. (2021). Geonomics: Forward-time, spatially explicit, and arbitrarily complex landscape genomic simulations. *Molecular Biology and Evolution*, 38(10), 4634–4646. https://doi.org/10.1093/molbev/msab175
- Thurman, T. J., & Barrett, R. D. H. (2016). The genetic consequences of selection in natural populations. *Molecular Ecology*, 25(7), 1429–1448. https://doi.org/10.1111/mec.13559
- Vertacnik, K. (2020). Predicting patterns of gene family evolution in taxa with similar ecological niches (University of Kentucky). University of Kentucky, https://doi.org/10.13023/etd.2020.371
- Vertacnik, K. L., & Linnen, C. R. (2015). Neodiprion lecontei genome assembly Nlec1.0. NCBI/GenBank. doi: https://doi.org/10.15482/USDA. ADC/1235565
- Via, S. (2001). Sympatric speciation in animals: the ugly duckling grows up. Trends in Ecology & Evolution, 16(7), 381–390. https://doi.org/10.1016/S0169-5347(01)02188-7
- Via, S. (2009). Natural selection in action during speciation. *Proceedings* of the National Academy of Sciences, 106(Supplement 1), 9939–9946. https://doi.org/10.1073/pnas.0901397106
- Via, S. (2012). Divergence hitchhiking and the spread of genomic isolation during ecological speciation-with-gene-flow. *Philosophical Transactions of the Royal Society B: Biological Sciences*, 367(1587), 451–460. https://doi.org/10.1098/rstb.2011.0260
- Via, S., & West, J. (2008). The genetic mosaic suggests a new role for hitchhiking in ecological speciation. *Molecular Ecology*, 17(19), 4334–4345. https://doi.org/10.1111/J.1365-294X.2008.03921.X
- Vicoso, B., & Charlesworth, B. (2006, August). Evolution on the X chromosome: Unusual patterns and processes. *Nature Reviews Genetics*, 7(8), 645–653. https://doi.org/10.1038/nrg1914
- Vicoso, B., & Charlesworth, B. (2009). Effective population size and the Faster-X effect: an extended model. *Evolution*, 63(9), 2413–2426. https://doi.org/10.1111/j.1558-5646.2009.00719.x
- Werren, J. H. (1993). The evolution of inbreeding in haplodiploid organisms. In N. Thornhill (Ed.), The Natural History of Inbreeding and Outbreeding: Theoretical and Empirical Perspectives. University of Chicago Press.

- White, N. J., & Butlin, R. K. (2021). Multidimensional divergent selection, local adaptation, and speciation. Evolution, 75(9), 2167–2178. https://doi.org/10.1111/evo.14312
- Wilfert, L., Gadau, J., & Schmid-Hempel, P. (2007). Variation in genomic recombination rates among animal taxa and the case of social insects. *Heredity*, *98*(4), 189–197. https://doi.org/10.1038/si.hdv.6800950
- Wilson, L. F., Wilkinson, R. C., & Averill, R. D. (1992). Redheaded pine sawfly: its ecology and management. U.S. Dept. of Agriculture, Forest Service.
- Wood, D. E., & Salzberg, S. L. (2014). Kraken: Ultrafast metagenomic sequence classification using exact alignments. *Genome Biology*, 15(3), R46. https://doi.org/10.1186/gb-2014-15-3-r46
- Wright, A. E., Harrison, P. W., Zimmer, F., Montgomery, S. H., Pointer, M. A., & Mank, J. E. (2015). Variation in promiscuity and sexual selection drives avian rate of Faster-Z evolution. *Molecular Ecology*, 24(6), 1218–1235. https://doi.org/10.1111/mec.13113
- Yeaman, S., Aeschbacher, S., & Bürger, R. (2016). The evolution of genomic islands by increased establishment probability of linked alleles. *Molecular Ecology*, 25(11), 2542–2558. https://doi.org/10.1111/mec.13611
- Yeaman, S., & Whitlock, M. (2011). The genetic architecture of adaptation under migration-selection balance. *Evolution; International Journal of Organic Evolution*, 65(7), 1897–1911. https://doi.org/10.1111/J.1558-5646.2011.01269.X

SUPPORTING INFORMATION

Additional supporting information may be found in the online version of the article at the publisher's website.

How to cite this article: Bendall, E. E., Bagley, R. K., Sousa, V. C., & Linnen, C. R. (2022). Faster-haplodiploid evolution under divergence-with-gene-flow: Simulations and empirical data from pine-feeding hymenopterans. *Molecular Ecology*, 31, 2348–2366. https://doi.org/10.1111/mec.16410